International Journal of Fracture Mechanics, Vol 5, No. 3, September 1969
Wolters-Noordhoff Publishing – Groningen
Printed in the Netherlands

Criteria for Crack Extension in Cylindrical Pressure Vessels

G. T. HAHN, M. SARRATE, AND A. R. ROSENFIELD*

Metal Science Group, Battelle Memorial Institute, Columbus Laboratories, Columbus, Ohio 43201

(Received September 11, 1968; in revised from February 28, 1969)

ABSTRACT

This paper describes three closely related criteria for the extension of axial through-cracks in cylindrical pressure vessels: (1) a fracture-toughness criterion mainly for low- and medium-tough materials, (2) a plastic flow stress criterion for short cracks in tough materials, and (3) a modification of (1) for relatively thin-walled containers. The development couples the Folias theoretical treatment of a pressurized cylindrical shell with the fracture-toughness approach and a new plasticity correction. This correction, which is consistent with crack-tip displacement measurements, shows that the plastic-flow strength governs the extension of short cracks in vessels fabricated from tough materials. This is to be contrasted with the behavior of longer cracks or more brittle materials which depends on the fracture toughness. The formulation is extended to vessels with large radius to wall-thickness ratios, e.g., $R/t > 50$ by way of a simple empirical modification. In this way, estimates of critical hoop stress-crack length combinations can be derived from the vessel radius to wall-thickness ratio, and either the ordinary yield strength, the yield and ultimate strengths, or K_c without prior full-scale test experience. Such estimates are shown to be in accord with the large body of published data encompassing ductile-steel, brittle-steel, as well as aluminum- and titanium-alloy vessels.

1. Introduction

The driving force for crack extension in a pressure vessel has two components: one is associated with the hoop stress, the second is a consequence of the radial pressure which tends to bulge the unsupported vessel wall adjacent to a through-crack. The radial-pressure component has no counterpart in the flat-plate test, but in a vessel it can make an even larger contribution to the crack-driving force than the hoop stress. Peters and Kuhn [1] devised a simple scheme for dealing with the two components that has since been given theoretical backing by Folias [2]. The basic premise is that a cylindrical pressure vessel can be treated like a flat panel (of the same material, thickness, and containing the same through-crack as the vessel) loaded in simple tension provided the nominal stress on the panel σ is taken to be a multiple M of the hoop stress σ_H**:

$$\sigma = M\sigma_H \,, \tag{1}$$

where M is a function of the crack length $2c$, the vessel radius r, and the wall thickness t. The critical hoop stress for crack extension in the pressure vessel σ_H^* can thus be described in terms of σ^*, the nominal stress for crack extension in the flat plate:

$$\sigma_H^* = \sigma^* M^{-1} \,. \tag{2}$$

Various proposals for the form of M for axial through-cracks in cylindrical vessels are summarized in Table 1. Expressions A, C, D, and E are based on experiments while expression B is derived from a theoretical analysis by Folias [2].

Anderson and Sullivan [3] enhanced the versatility of the approach by making it possible to draw on the larger body of fracture toughness data existing for flat plates. They coupled equation (2) with linear elastic fracture mechanics by replacing σ^* (which depends on crack length) with the fracture toughness parameter K_c (which is independent of crack length):

* The authors are associated with Battelle Memorial Institute, Columbus, Ohio, with M. Sarrate on leave of absence from the Argentine Atomic Energy Commission. This paper is scheduled for the 1969 WESTEC Conference, Los Angeles, California, 10–13 March.

** A complete list of symbols and definitions is in Appendix A.

$$\sigma_H^* = \frac{K_c}{(\pi c\varphi)^{\frac{1}{2}}} M^{-1}, \tag{3}$$

The factor $\varphi = \varphi(\sigma^*/\bar{\sigma})$ is a plasticity correction to the linear elastic fracture mechanics, which becomes significant when $\sigma^*/\bar{\sigma} \gtrsim 0.6$, where $\bar{\sigma}$ is the average plastic flow stress for the material. It should be noted here that K_c varies with plate thickness [8] and that the K_c-value inserted in equation (3) must be consistent with the wall thickness of the pressure vessel. If the fracture toughness is not known for a flat plate of the same thickness as the wall of the pressure vessel, an appropriate thickness correction should be made to the value of K_c used in equation (3).

TABLE 1.
*Criteria for crack extension in unstiffened cylindrical pressure vessels with axial through-cracks**

	Failure criterion	M	φ	Investigators
A	$\sigma_H^* = \sigma^* M^{-1}$	$\left[1+9.2\frac{c}{R}\right]$	—	Peters and Kuhn, 1957 [1]
B	$\sigma_H^* = \sigma^* M^{-1}$	$\left[1+1.61\left(\frac{c^2}{R^2}\right)\frac{R}{t}\right]^{\frac{1}{2}}$	—	Folias, 1965 [2]
C	$\sigma_H^* = \frac{K_c}{(\pi c\varphi)^{\frac{1}{2}}} M^{-1}$	$\left[1+\frac{\beta c}{R}\right]$	$\left[1+\frac{(M\sigma_H^*)^2}{2\sigma_Y^2}\right]$	Anderson and Sullivan, 1966 [3]
D**	$\sigma_H^* = \{\sigma_Y^4 \sigma_U^4 (g+hW)\}^{\frac{1}{2}} M^{-1}$	$[c^{\frac{1}{2}}]$	—	Nichols, Irvine, Quirk and Bevitt, 1965 [4]
E	$\sigma_H^* = \sigma^* M^{-1}$	$\left[1+\frac{c^2}{4Rt}\right]$	—	Kihara, Ikeda and Iwanga, 1966 [5]
F	$\sigma_H^* = \sigma^* M^{-1}$	$\left[1+0.81\left(\frac{c}{(Rt)^{\frac{1}{2}}}\right)\right]^{0.75}$	—	Crichlow and Wells, 1967 [6]
G	$\sigma_H^* = \frac{K_c}{(\pi c\varphi)^{\frac{1}{2}}} M^{-1}$	$\left[1+1.61\frac{c^2}{Rt}\right]^{\frac{1}{2}}$	$\left[\sec\frac{\pi\sigma_H^*}{(\sigma_Y+\sigma_U)}\right]$	Duffy, McClure, Eiber and Maxey, 1967 [7]

* A complete list of symbols and their definitions appears in Appendix A.
** Nichols *et al.* [4] give the relation in the following form: $\sigma_H^3 c^2 = \text{Const.}$

Duffy, McClure, Eiber, and Maxey [7] obtained a useful expression of these concepts by coupling (i) the Folias' equation for M (item B in Table 1), (ii) the fracture mechanics idea, and (iii) an estimate of φ derived from the Dugdale crack model. Their expression (Criterion G, Table 1) facilitates the prediction of burst pressures because the two material parameters involved, K_c and $\bar{\sigma}$ are well defined and, in principle, can be measured independently. In fact, the predictions made in this way by Duffy *et al.* [7] are in accord both with 2014-T6 aluminum vessels tested by Getz *et al.* [9] and with their own extensive measurements on steel pipes.

However, Criterion G has certain limitations when it is applied to very tough materials such as the usual steel vessels and pipes at ambient temperatures where crack extension proceeds by the ductile shear mode.* In this case, valid flat-plate K_c-determinations require very large test pieces, *e.g.*, 10–15 ft. wide, and this makes the flat-plate test prohibitive. In the absence of a K_c-value, burst-pressure predictions cannot be made without a prior full-scale test of a vessel. Predictions for short cracks in tough materials also involve very large plasticity corrections which are uncertain. Another problem is encountered when Criterion G is applied to relatively thin-walled nonferrous vessels, *e.g.*, $R/t > 100$. Contrary to the Folias analysis and experience with thicker steel vessels [5], [7], the M-values for the thin-walled vessels appear to be independent of thickness [1], [3].

* At least initially.

In the long term, solutions to these problems will be drawn from more rigorous elastic-plastic treatments of a cracked pressure vessel along the lines begun by Sechler and Williams [10] and Folias [2].

This paper offers two suggestions for improving the description by Duffy and co-workers. An alternative, in part a more rigorous plasticity correction based on crack-tip displacement, is identified. When this correction is employed it becomes apparent that the fracture toughness plays a minor role in the extension of short cracks in tough materials. In this case, a measure of the toughness is not needed and failure pressures can be estimated directly from either the ordinary yield strength or yield and ultimate strength values. However, the K_c-value does influence the performance of vessels with long cracks and those constructed of more brittle materials. The wall-thickness discrepancies are dealt with by modifying the Folias expression for M empirically. The resulting criteria for crack extension are shown to be in accord with the large body of published data on pressure vessels.

2. The Plasticity Correction

A brief discussion of the significance of K_c and φ appears in Appendix B. Previous workers have evaluated φ by way of the simplifying assumption that the plastic zone supports no stress and can be treated like an extension of the crack. Anderson and Sullivan [3] obtain their correction, referred to as φ_1, from a zone-size estimate based on the linear elastic stress-field solution, an approximation which is not sound at high stress levels. The Duffy *et al.* [7] correction, φ_2 is more meaningful at higher stresses because its size estimate is drawn from Dugdale's [11] elastic-plastic model. However, their procedure still overestimates the value of φ since the plastic zone really supports stresses comparable to the flow strength of the material. A more realistic treatment that is based on the distortion at the crack tip and accounts for the stress supported by the plastic zone in a flat plate is given in Appendix B and leads to equation (B.7).

These plasticity corrections are derived from analyses of flat plates. To make the transition to a cylindrical vessel σ^*, the flat-plate failure stress must be replaced by $\sigma_B^* \cdot M$, a procedure consistent with the sense of equation (1)*, and adopted previously by Anderson and Sullivan

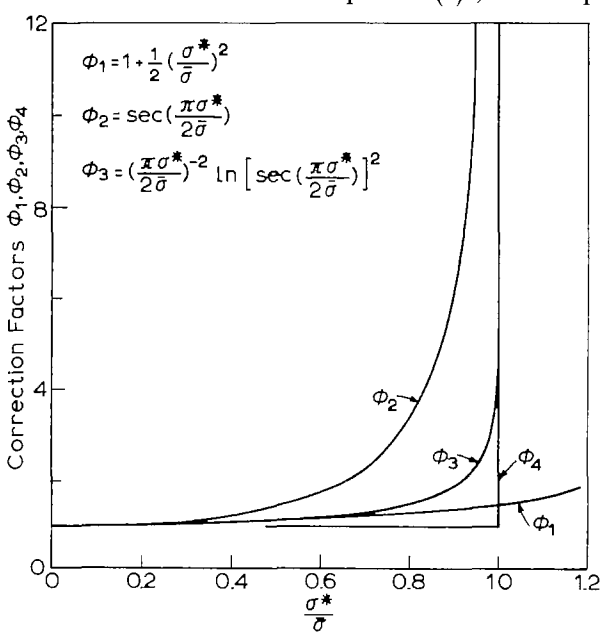

Figure 1 Comparison of plastic-zone corrections evaluated for flat plates · φ_1 is the form employed by Anderson and Sullivan [3], φ_2 by Duffy *et al.* [7], and φ_3 and φ_4 in the present study. Note that the relative positions of the curves are changed when the corrections are applied to cylindrical vessels.

* The pressure vessel behaves like a flat plate loaded to a stress $\sigma = M\sigma_B$.

(Table 1). Accordingly:

$$\varphi_3 = \left(\frac{\pi M \sigma_H^*}{2\bar{\sigma}}\right)^{-2} \ln\left[\sec\frac{\pi M \sigma_H^*}{2\bar{\sigma}}\right]^2 . \tag{4}$$

The quantity $\bar{\sigma}$ must be interpreted as an average flow stress acting in the plastic zone, and can not be precisely defined. At low nominal stresses the plastic strains generated in the zone are small, and $\bar{\sigma}=\sigma_Y$ (σ_Y is the yield stress) is probably a good estimate. At higher stress levels the influence of strain hardening is felt, and $\bar{\sigma}>\sigma_Y$, with $\bar{\sigma}=\sigma_U$ (σ_U is the ultimate tensile strength) an approximate upper limit. The two limits are used here because they probably bracket the true correction and reflect the inherent uncertainty of this part of the analysis:

$$\varphi_3(\bar{\sigma}=\sigma_Y) < \varphi < \varphi_3(\bar{\sigma}=\sigma_U) . \tag{5}$$

Figure 1 compares the three corrections as evaluated for flat plates and shows that φ_2 is larger than either φ_1 or φ_3 (for a given value of $\sigma^*/\bar{\sigma}$). Figure 2 shows that the positions are

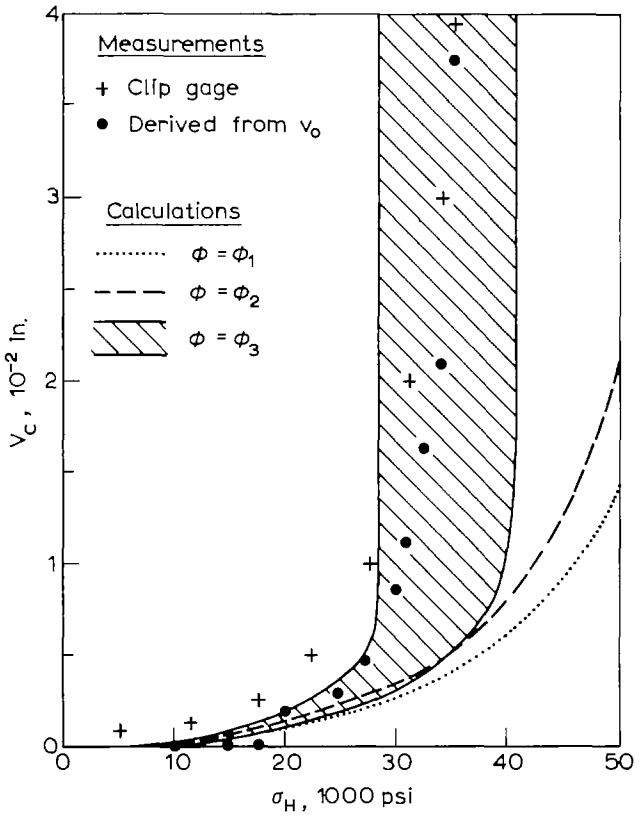

Figure 2. Comparison of crack-tip displacement measurements with calculations based on φ_1, φ_2, and φ_3. The measurements were performed on a 5-in.-internal diameter, 0.5-in.-thick mild steel vessel ($\sigma_Y=45.7$ ksi, $\sigma_U=66$ ksi). The calculations employ the following relations: $v_c=\pi B c\sigma^2\varphi$, $\sigma=\sigma_H M$, and the different expressions for φ.

reversed when the corrections are applied to cylindrical vessels. This arises because Duffy *et al.* [7] equate the critical flat-plate stress with the critical hoop stress: $\sigma^* \equiv \sigma_H^*$ while Anderson and Sullivan [3] and the present authors take $\sigma^* \equiv M\sigma_H^*$. Also note that different definitions of $\bar{\sigma}$ are involved; Anderson and Sullivan: $\bar{\sigma}=\sigma_Y$, Duffy *et al.* $\bar{\sigma}=\frac{1}{2}(\sigma_Y+\sigma_U)$, and the present authors: $\sigma_Y<\bar{\sigma}<\sigma_U$. As a result, φ_3 is similar to φ_2 at low-stress levels, but much larger at high-stress levels because $\varphi_3\to\infty$ as $\sigma_H\to\bar{\sigma}/M$, while $\varphi_2\to\infty$ as $\sigma_H^*\to\bar{\sigma}$. The crack-tip displacement values derived from the work of Almond *et al.* [12], which are reproduced in Fig. 2, provide direct experimental evidence in support of the formulation of φ_3*. The values were ob-

* As noted in Appendix B.1, v_c, the crack opening displacement is also a function of the plasticity correction: $v_c=(\sigma^2\pi c/2E\bar{\sigma})\varphi$, where σ is the flat plate nominal stress ($\sigma=M\sigma_H$), $2c$ is the crack length, E is the elastic modulus, and $\bar{\sigma}$ is the average flow stress. Thus, measurements of v_c can provide a direct check of the value of φ.

tained from two sources: (1) directly, from clip-gage measurements at the crack tip, and (2) indirectly, from crack center displacement values* and equation (B.11). Figure 2 shows that v_c, the crack tip displacement increases very rapidly in pressurized pipes at stresses in the range $\sigma_Y < M\sigma_H < \sigma_U$. Calculated curves based on the maximum and minimum values of φ_3 bracket the measurements, while calculations based on φ_1 and φ_2 do not reproduce the trends observed. The rapid increase of v_c as $\sigma_H \to \bar{\sigma}/M$, revealed in Fig. 2, is attributed to a gross distortion of the region surrounding the crack to which bulging probably contributes. It cannot be identified with the general yielding of the pressure vessel that occurs when $\sigma_H \to \bar{\sigma}$. To draw attention to this distinction, the phenomenon is referred to as "large-scale yielding" in this paper.

3. Criteria for Crack Extension

When the new plasticity correction is coupled with the Folias expression for M and a modification of it to be discussed, a criterion for the extension** of through-cracks in three categories of vessels emerges. The three categories are described in Table 2. In each case, the criterion assumes a slightly different form, and these are derived and compared with actual measurements in the following sections.

Category 1. *Intermediate wall thickness, low-to-medium-toughness vessel with relatively long cracks*

TABLE 2

Criteria for the extension of axial through-cracks in unstiffened pressure vessels

Category	Specifications $\frac{R}{t}\left(\frac{K_c}{\sigma_Y}\right)^2\frac{1}{c}$		Criterion	M	Applications
1. Intermediate wall thickness, low-to medium-toughness vessels with relatively long cracks	5–50	<7	$\sigma_H^* = \dfrac{K_c}{(\pi c\varphi_3)^{\frac{1}{2}}} M^{-1}$	$\left[1+1.61\dfrac{c^2}{Rt}\right]^{\frac{1}{2}}$	Steel pipe lines and pressure vessels operating below the shear-to cleavage-fracture transition temperature
2 Intermediate wall thickness high-toughness vessels with relatively short cracks	5–50	>7	$\sigma_H^* = \bar{\sigma}M^{-1}$ and $\bar{\sigma}(\text{ksi}) = 1.04\sigma_Y(\text{ksi}) + 10.0$ $\bar{\sigma}(\text{ksi}) = 1.23\sigma_Y(\text{ksi})$ $\bar{\sigma}(\text{ksi}) = 0.66[\sigma_Y(\text{ksi}) + \sigma_U(\text{ksi})] - 18.1$ $\bar{\sigma}(\text{ksi}) = 0.51[\sigma_Y(\text{ksi}) + \sigma_U(\text{ksi})]$	$\left[1+1.61\dfrac{c^2}{Rt}\right]^{\frac{1}{2}}$	Steel pipe lines and pressure vessels that fail by 100% shear fracture
3 Very thin wall, low and medium toughness vessels with relatively long cracks	>50	>7	$\sigma_H^* = \dfrac{K_c}{(\pi c\varphi_3)^{\frac{1}{2}}} M^{-1}$	$\left[1+1.61\dfrac{c^2}{R^2}\left(50\tanh\dfrac{R}{50t}\right)\right]^{\frac{1}{2}}$	Thin walled rocket propellant tanks

R Vessel radius
t Wall thickness
$2c$ Crack length
K_c Fracture toughness
σ_H^* Critical hoop stress
σ_U Ultimate tensile stress
$\bar{\sigma}$ Average flow stress. Note that more than one definition of $\bar{\sigma}$ is used. The value of $\bar{\sigma}$ appropriate for the failure criterion of Category 2 vessels is reasonably well established only for low- and medium-strength steel vessels. The value of $\bar{\sigma}$ to be inserted into φ_3 cannot be defined as precisely. At present, only the following estimates of the upper and lower bound are employed $\sigma_Y < \bar{\sigma} < \sigma_U$.
φ_3 Plasticity correction

$$\begin{cases} \varphi_3 = \left(\dfrac{\pi\sigma_H^* M}{2\bar{\sigma}}\right)\ln\left[\sec\dfrac{\pi\sigma_H^* M}{2\bar{\sigma}}\right] \\ \sigma_Y < \bar{\sigma} < \sigma_U \end{cases}$$

* Taken from photographs of the pressurized containers made available to the present authors.
** The term crack extension is used in this paper to denote the onset of unstable crack extension (or fast fracture) as opposed to an onset of stable crack growth.

Inserting φ_3 and the Folias expression for M into equation (3) leads to the following criterion:

$$\sigma_H^* = \frac{K_c}{(\pi c \varphi_3)^{\frac{1}{2}}} \left[1 + 1.61 \frac{c^2}{Rt}\right]^{-\frac{1}{2}} . \tag{6}$$

While this expression should be generally valid for wall thicknesses in the range $5 < (R/t) < 50$, a simpler expression is derived in the next section for high-toughness vessels with short cracks. In view of this, equation (6) can be restricted to the range $(K_c/\sigma_Y)^2 c^{-1} < 7$, which encompasses low- to medium-toughness vessels with relatively long cracks.

Inspection of equation (6) reveals that $(\sigma_H^2 \pi c \varphi_3)^{-1}$ is a linear function of (c^2/Rt) with $(K_c)^{-2}$ and $1.61\,(K_c)^{-2}$, the intercept and slope respectively. A graphical presentation of data in this form offers a convenient test of the criterion; such a presentation shows (i) whether the expected linear relation is obeyed, and (ii) whether the intercept and slope agree. The K_c-value that agrees best with the slope and intercept can then be compared with flat plate measurements.

Figures 3 and 4 show that the results of all previous experiments in this category* are in reasonably good accord with the failure criterion. In each case the results can be approximated

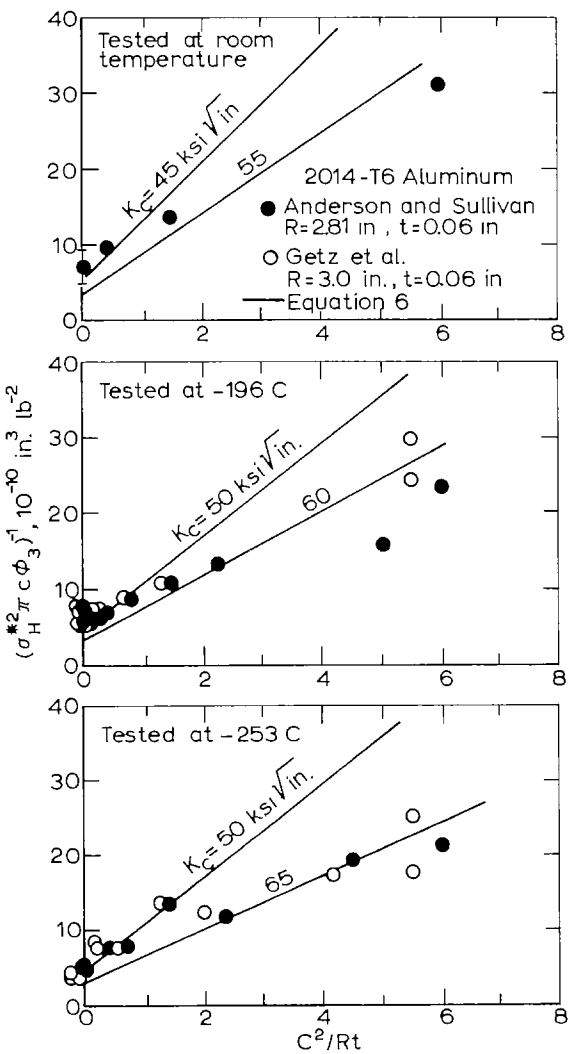

Figure 3. Comparison of pressure-vessel crack-extension measurements performed by Anderson and Sullivan [3] and Getz *et al.* [9] on 2014-T6 aluminum with lines calculated from equation (6) Room temperature (top), −196°C (middle), −253°C (bottom)

* Complications of all the data are given in Appendix D.

by a linear relation with a slope and intercept consistent with a single value of K_c. Furthermore, Table 3 illustrates that these K_c-values agree with the values derived from flat-plate tests. The pressure-vessel data for 2014-T6 alloy are drawn from two sources and agree very well, but the flat-plate results reported by the same investigators do not agree. Anderson and Sillivan [2] find that the flat-plate K_c-value decreases as the temperature is lowered. On the other hand, Getz *et al.* [9] report evidence that K_c increases below room temperature. Thus, Table 2 shows that the K_c-values deduced from the modified criterion fall somewhere between these expectations. The K_c-values derived from the Kihara *et al.* measurements on steel at -196 C are in excellent agreement with flat-plate values obtained on the same material at the same temperature. The agreement is especially significant because the Kihara results are the only systematic measurements reported so far on crack extension by "brittle" cleavage. The results obtained by Nichols *et al.* [4] on the 0.36 percent carbon steel vessels (see Fig. 4) tested at temperatures where the steel behaves in a semibrittle fashion are also in accord with flat-plate tests.* Both

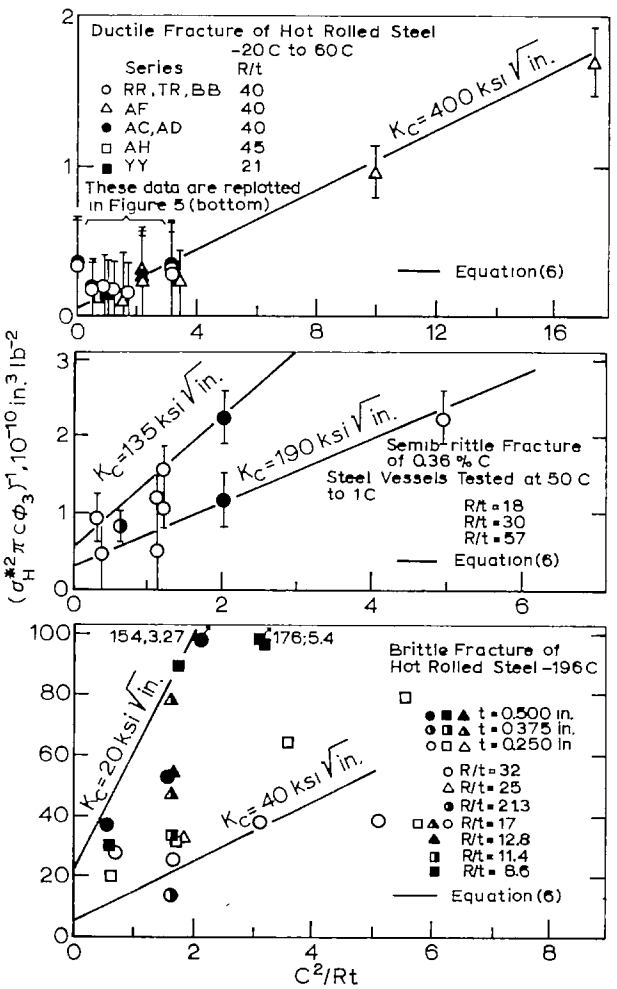

Figure 4 Comparison of the crack-extension behavior of hot-rolled steel vessels with equation (6). Ductile crack extension studied by Duffy, *et al.* [7] (top), semibrittle extension by Nichols, *et al.* [4] (middle), brittle extension by Kihara, *et al.* [5] (bottom).

* The interpretation of the results of Nichols *et al.* [4] is complicated because their vessels and flat plates were tested over a temperature range that encompasses both ductile and brittle behavior and because the data for vessels and plates of the same material do not reflect the same test temperatures. However, their results are especially important because they afford the only relatively direct comparison with flat plates having dimensions (7 ft. wide) that approach those capable of yielding meaningful K_c-values for hot rolled steel in the ductile condition. Since these K_c-values are not quoted by Nichols *et al.* [4], they are listed and identified in Appendix C, Table C-2.

TABLE 3

Comparison of the average flow stress and the K_c-values deduced from pressure vessel tests with values obtained from tensile tests or flat-plate experiments

Category 1. Vessels Material and test conditions	R/t	K_c, ksi $\sqrt{\text{in.}}$	
		Pressure vessel test (Equation 6)	Flat plate fracture toughness test
Hot rolled steel [4]; 0.36 C steel, vessels tested at 1–50°C and displayed mixed-mode fracture (a)	18–57	135–190	120–160 [4], [6]
Hot rolled steel [5]; 0.23 C steel, vessels tested at −196°C and displayed cleavage fracture	8–23	20–40	20–35 [5], [13]
2014-T6 Aluminum [3], [9]			
RT	47	45–55	58 [3]
−196°C	47–50	50–60	49 [3], >58 [9]
−253°C	47–50	50–65	44 [3], >58 [9]

TABLE 3

(*Continued*)

Category 2. Vessels. Material and test conditions	$\frac{R}{t}$	$\bar{\sigma}$ ksi		
		Derived from pressure vessel test data (σ_H^*, eq. 7)	Derived from tensile test data (σ_T, eq. 8A)	Derived from tensile test data (σ_T, σ_U, eq. 8B)
Hot rolled steel [7]; a series of line pipe steel, vessels tested in the range 20–60°C and displayed full-shear fracture (a)				
Series RR, T4, BB	40	72	73	74
Series AF	40	80	81	82
Series AC, AD	40	69	69	68
Series UU	12	84	74	69
Series GP	46	75	63	64
Series AH	45	70	71	73
Hot rolled steel [4]; 0 36 C steel, vessel tested at 62–88°C and displayed full-shear fracture (a)	30	44	46	50
0.16 C, Si-killed steel vessel tested at 39°C and displayed full-shear fracture (a)	30	45	42	44
0.13 C, Al-grain refined steel, vessels tested at 16–79°C and displayed full-shear fracture (a)	30	55	52	50
Hot rolled steel [12]; 0.14 C steel, vessels tested at −120 to 25°C and displayed full-shear fracture (a)				
25°C	5	55	57	56
−5 to 5°C	5	60	59	59
−68°C	5	69	61	65
−120°C	5	71	78	83

TABLE 3
(*Continued*)

Category 3. Vessels Material and test conditions	R/t	K_c ksi $\sqrt{\text{in.}}$	
		Pressure vessel test (Equation 9)	Flat plate fracture toughness test
5A1-2.5 Sn Titanium [3];			
$-196°C$	150	150	140 [3]
$-253°C$	150	100	88 [3]
2024-T3 Aluminum [1]			
RT	144–960	50–80	60–80 [14][c]
7075-T6 Aluminum [1]	144–900	30–40	53–58 [14][c]
8A1-IV-1Mo Titanium [6]	300–2300	~150	~100[d]

[a] Refers to the initial mode of crack extension.
[b] See Appendix C, Table C.2.
[c] These values were obtained on 0.060 in.-thick sheet, while the pressure vessels were fabricated from 0.006 in.-0.025 in.-thick sheet. The higher gages would be expected to display smaller K_c-values [8].
[d] This estimate is based on $2 \cdot K_{Ic}$ [15], [16].

the Nichols *et al.* and the Kihara *et al.* data display much scatter, but this is no larger than the scatter displayed by the corresponding flat-plate tests.* The scatter may be aggravated by the problem of sealing the longer cracks against pressure loss without stiffening and thereby strengthening the vessel wall. Systematic deviations from linearity evident in Fig. 3 may be a manifestation of this. It should also be noted that in each case two values of the parameter $(\sigma_H^{*2} \pi c \varphi_3)^{-1}$ were calculated corresponding to the two limiting values of φ_3 (for $\bar{\sigma} = \sigma_Y$ and $\bar{\sigma} = \sigma_U$). The divergence, which is indicated by brackets whenever significant (see Fig. 4), reflects the uncertainties in the treatment of the plasticity correction rather than in the measurements themselves. The correction is especially uncertain when applied to short cracks in ductile steel pipes (Fig. 4, top), cases where $(K_c/\sigma_Y)^2 c^{-1} > 7$, and which lend themselves to the simpler criterion described in the next section. Results for the two longest cracks tested by Duffy *et al.* provide a basis for assigning a value of $K_c = 400$ ksi $\sqrt{\text{in.}}$ to the toughness of X-60 pipeline steel in the fully ductile condition. This value compared favorably with a lower limit, $K_c > 305$–432 ksi $\sqrt{\text{in.}}$, derived from flat-plate tests of a hot-rolled steel in the fully ductile condition by Nichols *et al.* (see Table C-2).

Category 2. High-toughness vessels with short cracks

Figure 1 illustrates that at high stress levels when σ^* (or equivalently $M\sigma_H^*$) approach $\bar{\sigma}$, φ_3 becomes a rapidly varying function of $\bar{\sigma}$. As a result, the plasticity correction dominates the failure criterion and equation (6) reduces to a simpler form. This is seen by noting that φ_3 is closely approximated by a simple step function φ_4, shown in Fig. 1. When φ_4 is substituted for φ_3, equation (6) reduces to:

$$\sigma_H^* = \bar{\sigma} \left(1 + 1.61 \frac{c^2}{Rt}\right)^{-\frac{1}{2}}, \tag{7}$$

The fracture-toughness criterion thus reduces to a flow-stress criterion an indication that "large-scale yielding" is the load-limiting process. Equation (7) should be a valid criterion when $\varphi_3 \approx \varphi_4$, or when $\sigma_H^* M \gtrsim 0.9\,\sigma$ and $\varphi_3 \gtrsim 2$ (see Fig. 1). By combining these limits with equation (3) and the approximation $\bar{\sigma} \approx 1.2\sigma_Y$, it develops that the flow stress criterion is valid when $(K_c/\sigma_Y)^2 c^{-1} \gtrsim 7$, which restricts the criterion to relatively tough materials with short cracks.

* The Nichols *et al.* tests described in Fig. 4 were carried out in the transition-temperature range where K_c varies markedly with the temperature. The Kihara *et al.* data show systematic variations of K_c with plate thickness. Flat-plate test data obtained by these investigators are summarized in Appendix C.

According to equation (7), σ_H^{*-2} should be a linear function of (c^2/Rt) with $\bar{\sigma}^{-2}$ and $1.61\bar{\sigma}^{-2}$ as the intercept and slope, respectively. Figure 5 and Table 3 illustrate that the results of three major studies encompassing six grades of hot-rolled steel and a wide range of vessel geometries tend to satisfy this requirement. Regression analyses of the 45 data points in Fig. 5 were con-

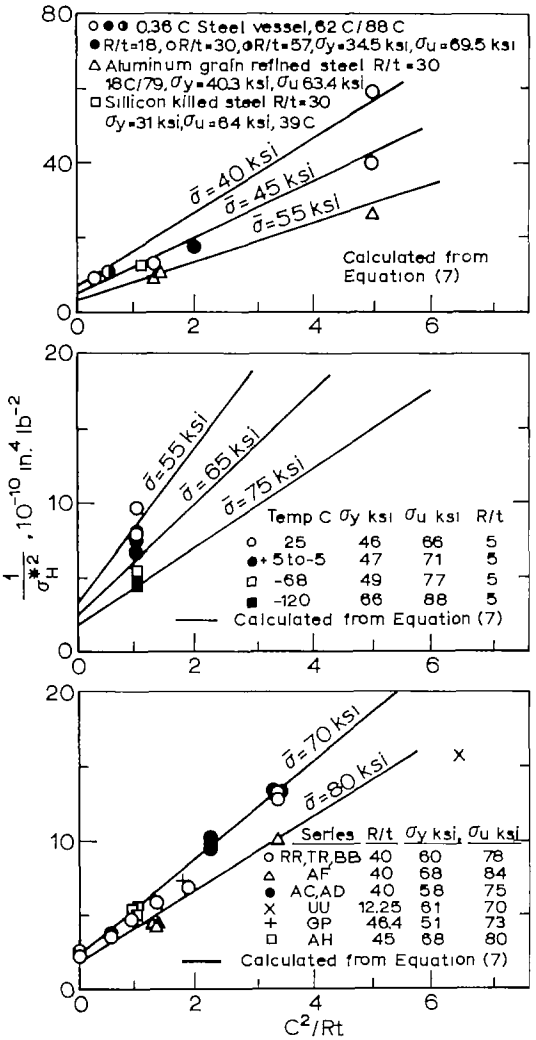

Figure 5. Comparison of the ductile crack-extension behavior of hot-rolled steel pressure vessels with equation (7). Data of Nichols *et al.* [4] (top), Almond *et al.* [12] (middle), Duffy *et al.* [7] (bottom).

ducted and these show that $\bar{\sigma}$ correlates with both σ_Y or $(\sigma_Y+\sigma_U)^\star$:

	Standard error of estimates, ksi	Percent explained variation	
$\bar{\sigma}\,(\text{ksi}) = 1.04\sigma_Y(\text{ksi}) + 10.0$	4.76	84	(8a)
$\bar{\sigma}\,(\text{ksi}) = 1.23\sigma_Y(\text{ksi})$	5.20	81	(8b)
$\bar{\sigma}\,(\text{ksi}) = 0.66[\sigma_Y(\text{ksi}) + \sigma_U(\text{ksi})] - 18.1$	5.93	57	(8c)
$\bar{\sigma}\,(\text{ksi}) = 0.51[\sigma_Y(\text{ksi}) + \sigma_U(\text{ksi})]$	6.40	50	(8d)

⋆ Note that equations (8a)–(8d) are derived from data on low- and medium-strength steel vessels and do not necessarily describe $\bar{\sigma}$-values for other materials as accurately This especially is true for equations (8a) and (8b) which may reflect systematic changes in the stress-strain relations that are characteristic of these steels. Since equation (8c) contains both σ_Y and σ_U, it may be a better approximation than (8a) or (8b) for other materials even though it is a poorer description of the steels.

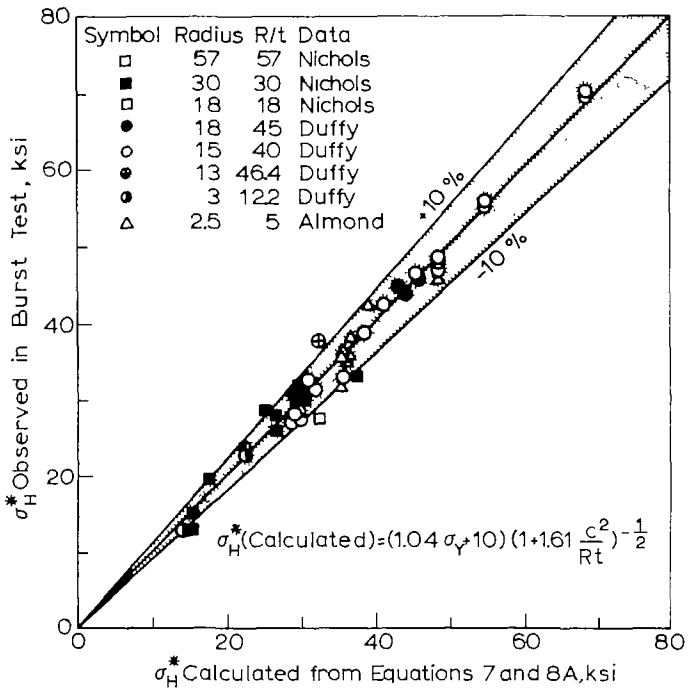

Figure 6. Comparison of the critical hoop-stress values calculated from equations (7) and (8a) with values observed in 45 different pressure-vessel tests.

Figure 6 compares the results of the 45 actual tests with predicted values of σ_H^U derived from equations (7) and (8a) and shows that 40 out of 45 predictions are accurate to within 10 percent.

Category 3. *Very thin walled vessels*

While equation (6) makes useful predictions for vessels of intermediate wall thicknesses from $5 < (R/t) < 50$, it fails to predict the results of four series of tests on very thin-walled vessels in the range $144 < (R/t) < 2500$ [2024-T3 Al, [1] 7075-T6 Al, [1] Ti-5Al-2. 5 Sn, [3] and Ti-8Al-1Mo-1V [6]]. These vessels behave as if M is independent of thickness—a conclusion reached earlier by Peters and Kuhn [1] and Anderson and Sullivan [3]. In other words, the vessels behave as if the R/t contribution to M (note that $(c^2/Rt) = (c^2/R^2)(R/t)$ saturates in the range $50 < (R/t) < 144$. This is consistent with Folias' own evaluation, namely, that his expression for M is limited to geometries where $c/Rt < 1$, which is equivalent to $(R/t) \lesssim 50$ because $(c/R) \gtrsim 0.15$ in most tests. Since the thickness effect is not likely to disappear abruptly, an attempt was made to describe a diminishing R/t contribution empirically. This can be done in the appropriate range by replacing R/t with the function $\lambda \tanh R/\lambda t$, where $\lambda = 50$:

$$\sigma_H^{*2} = \frac{K_c}{(\pi c \psi_3)^{\frac{1}{2}}} \left[1 + 1.61 \frac{c^2}{R^2} \left(50 \tanh \frac{R}{50t}\right)\right]^{-\frac{1}{2}}. \tag{9}$$

This form introduces no new undefined parameters and approximates equation (6) for $(R/t) < 50$.

Available test results are compared with this criterion in Fig. 7 and 8, again plotted so as to take advantage of a linear relation with an intercept and slope of K_c^{-2} and $1.61\, K_c^{-2}$, respectively. While the results for the thin vessels are more scattered than those for the heavier wall containers, the intercepts and slopes are roughly in accord both with equation (9), and with the flat-plate K_c-values summarized in Table 3. The K_c-values for the Ti-5Al-2.5 Sn alloy agree very well with flat-plate measurements on the same material. The K_c-value indicated by the measurements of the Ti-8Al-1Mo-1V alloy is not unreasonable although a direct comparison is not possible. The abnormally large σ_H^*-values (low σ_H^{*-2} values) for tests involving the longest cracks in this series of tests and some of the others are probably associated with the problem

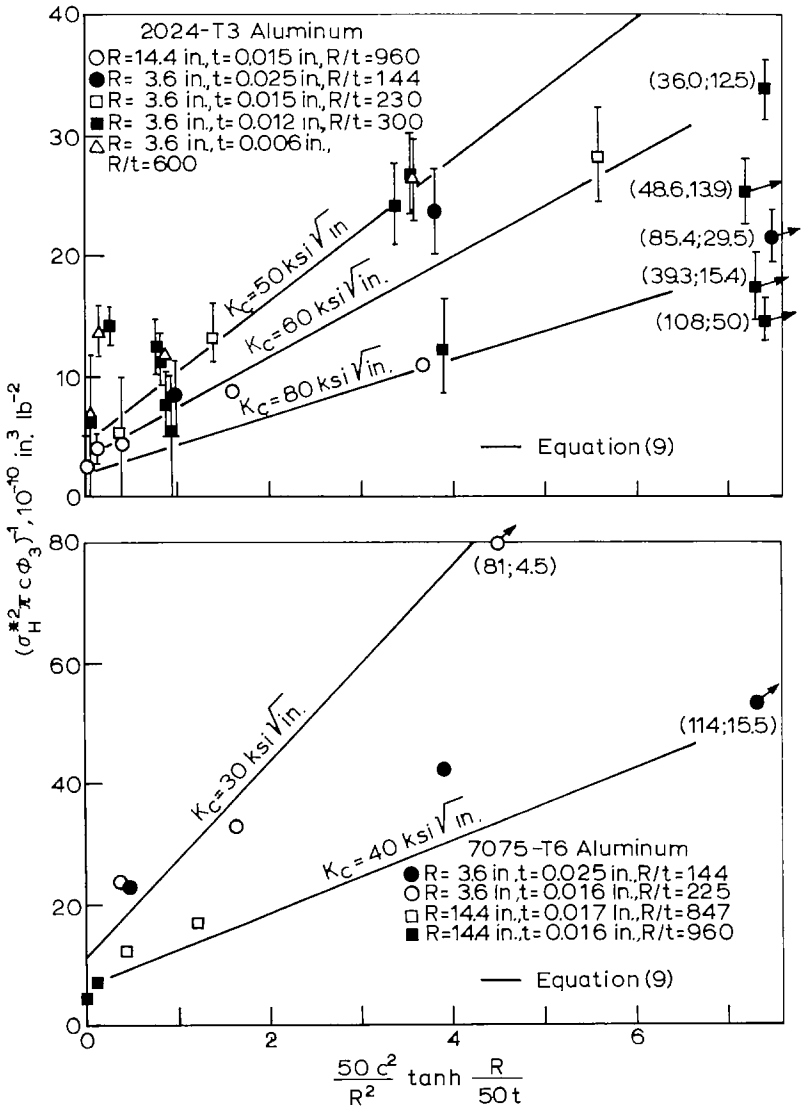

Figure 7. Comparison of pressure-vessel crack-extension measurements reported by Peters and Kuhn [1] with calculated lines derived from equation (9). 2024-T3 Aluminum (top), 7075-T6 Aluminum (bottom).

of sealing a crack without strengthening the configuration. The K_c-values derived from the 7075-T6 and 2024-T3, 0.006 to 0.025-in.-thick vessels are somewhat smaller than the values derived from Forman's [14] measurements on albeit heavier gage, 0.060-in.-thick panels.* However, the discrepancy is in the right direction and might vanish if the comparison were extended to even thinner panels. Test data reported by Sechler and Williams [10] for thin brass containers (t=0.001 to 0.003 in., R/t=833–2500) can also be fitted with equation (9) and a K_c-value of 25 ksi $\sqrt{\text{in.}}$, but there are no flat-sheet toughness values available for comparison.

4. Discussion

The three criteria for crack extension derived here contain several innovations. One is a new plasticity correction that is in accord with crack-tip displacement measurements. With this correction, a fracture-toughness criterion is obtained that at low hoop-stress levels makes

* The values cited by Anderson and Sullivan [3] as representative for these alloys: K_c (705-T6) = 53 ksi$\sqrt{\text{in.}}$, K (2024-T3) = 90 ksi$\sqrt{\text{in.}}$ probably reflect even heavier gages than those studied by Forman.

essentially the same predictions as the one proposed by Duffy *et al.* At high-stress levels the correction leads to a new concept, namely, that the extension of short cracks in tough vessels is controlled by the "large-scale yielding" and governed by a flow-stress criterion. The flow-stress criterion is important from a practical standpoint, first, because short cracks are more likely to escape detection than long ones. Second, the flow-stress criterion makes it possible to predict burst pressures in the absence of K_c-values for the very materials for which K_c is difficult to measure and not well known. The two facets of the plasticity correction also indicate that the crack-extension resistance of a vessel can best be improved:

(1) By raising the yield and ultimate tensile strength when

$$\left(\frac{K_c}{\sigma_Y}\right)^2 \frac{1}{c} > 7$$

(2) By enhancing the fracture toughness of the material when

$$\left(\frac{K_c}{\sigma_Y}\right)^2 \frac{1}{c} < 7 .$$

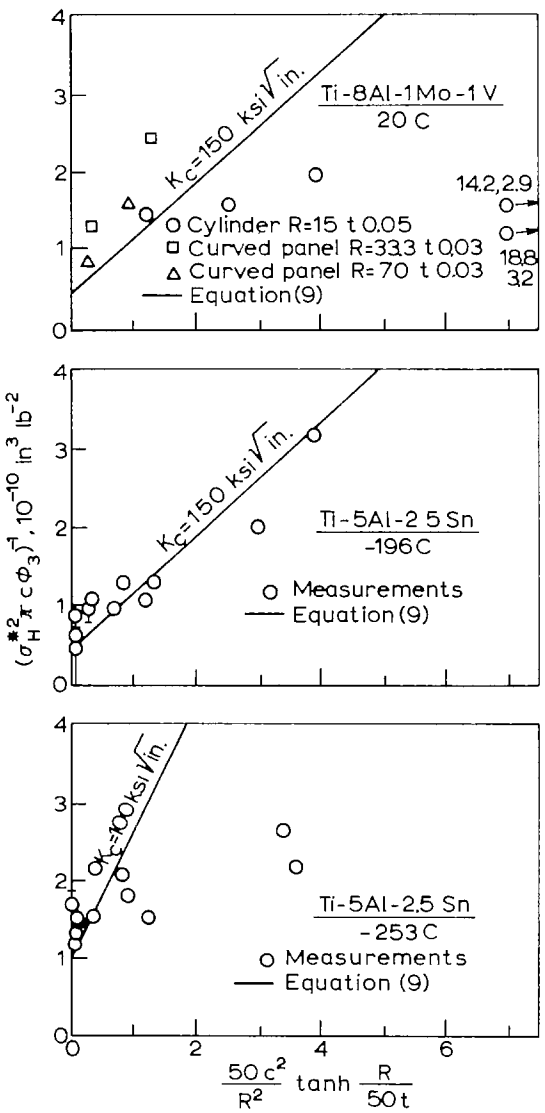

Figure 8. Comparison of pressure-vessel crack-extension measurements with equation (9). Ti-8Al-1Mo-IV data reported by Crichlow *et al.* [6] (top), Ti-5Al-2.5 Sn by Anderson and Sullivan [3] (middle and bottom).

This clarifies the metallurgy of the problem since composition and processing are not likely to affect $\bar{\sigma}$ and K_c in the same way. The tanh-modification extends the usefulness of the approach and points to an underlying connection between the results for medium- and very thin-walled vessels.

In fact, all three criteria are closely related—the first two are special forms of the third. Although other criteria can be fitted to some of the measurements with good precision, the present formulation allows the bulk of the data in the literature to be described reasonably successfully with essentially one expression that involves no undefined material or geometric parameters. Finally, this formulation lends itself to making of predictions. This is in contrast with the Criterion D, Table 1, proposed by Nichols *et al.* [4] which Quirk [17] has recently fitted to a wide range of pressure-vessel data. The Nichols *et al.* criterion does not explicity describe the contribution of vessel radius or wall thickness and involves three material constants and four disposable parameters.

Although significant agreements with experiment are cited, both the "large-scale yielding" idea and the tanh-modification need to be examined more critically. In the first case, M is derived from Folias' elastic treatment which is most vulnerable in the presence of gross yielding. Further work on this aspect of the problem will benefit from more systematic measurements of the distortions of a cracked vessel along the lines begun by Almond *et al.*, particularly the crack opening, the character of the bulge, and the extent of local plastic deformation. In the second case there is the possibility that the departures from a c^2/Rt-dependence displayed by very thin-walled vessels result wholly or in part from the added stiffness and strength conferred by the patch that seals the cracked vessel against pressure loss. Although the observed departures appear too systematic to be explained in this way, the effect of the patch has received little attention and cannot be discounted. More measurements on vessels fabricated from sheets and plates with well-established K_c-values are needed to fill the large gap that now exists between $50 < (R/t) < 150$, and to provide a more critical test of tanh-modification in the range $200 < (R/t) < 1000$. Studies of longer cracks, i.e., $(c/R) > 0.5$, are also desirable since the expressions for M used in both criteria are untested beyond this point. Information on long cracks is a prerequisite for treating crack propagation and the speed of failures in pressure vessels.

5. Conclusions

(1) Three closely related criteria for the extension of through-cracks in pressure vessels are derived: (i) a fracture-toughness criterion mainly for low- and medium-tough materials, (ii) a flow-stress criterion for short cracks in tough materials, and (iii) a modification of (i) for very thin vessels. The criteria make use of the Folias analysis for a pressurized cylindrical shell (the fracture toughness approach) and a plasticity correction based on the crack-tip displacement of the Dugdale crack model.

(2) The plasticity correction is small when failure occurs at relatively low hoopstress levels such as may be encountered with low- and medium-tough materials. In such cases, burst pressures can be estimated with a fracture-toughness criterion like the one devised by Duffy and coworkers which relies on a knowledge of K_c (the flat-plate fracture toughness of the material). The toughness criterion is shown to be in good accord with test experience for 2014-T6 aluminum as well as brittle and semibrittle steel vessels.

(3) The plasticity correction departs significantly at high hoop-stress levels from existing formulations. It suggests that in this range, cracked vessels undergo "large-scale yielding"—a phenomenon similar to "general yielding" in flat plates—and that this can occur while the hoop-stress level is still below the yield stress of material. The "large-scale yielding" concept also receives support from crack-tip displacement measurements on vessel and burst-pressure data.

(4) The fracture-toughness criterion reduces to a simpler flow-stress criterion at stress levels corresponding to "large-scale yielding". Accordingly, critical hoop-stress and burst-pressure predictions can be made for relatively short cracks in tough materials from a knowledge of ordinary yield and ultimate tensile strength values for materials, and without recourse to K_c.

Excellent predictions can be made in this way for virtually all steel vessels that have failed with full-shear fractures.
(5) A simple empirical modification of the Folias result which involves no additional undefined parameters offers the possibility of extending the validity of the fracture-toughness criterion to very thin walled vessels, *i.e.*, vessels with wall radius-to-thickness ratios in excess of 50. The modification appears to be in accord, at least approximately, with results for a wide range of thicknesses and geometries.

Note added in proof:
The readers' attention is drawn to the papers by Sanders and his associates which came to our attention after this manuscript was submitted. The papers appear on pages 117 and 133 of the *International Journal of Fracture Mechanics*, Vol. 5.

Acknowledgements

The authors are grateful to the American Gas Association for financial support. They wish to thank E. A. Almond for generously making available unpublished results of his work on pressure vessels, M. F. Kanninen for many useful contributions to the manuscript, and J. H. Broehl for assistance with the regression analyses. The authors are also indebted to A. R. Duffy, R. J. Eiber, W. A. Maxey for their fruitful discussions and cooperation, and to C. Pepper for her work on the manuscript.

Appendix A

List of symbols

B	Displacement coefficient $B \equiv 2E\bar{\sigma}$
c	Crack half length
e, f, g, h	Coefficients that depend on the geometry of the vessel
E	Young's modulus
K	Stress intensity parameter $K_c = \sigma(\pi c\varphi)^{\frac{1}{2}}$
K_c	Fracture toughness parameter $K_c = \sigma^*(\pi c\varphi)^{\frac{1}{2}}$
K_{Ic}	Plane strain fracture toughness parameter
M	Bulging factor. $M \equiv \sigma/\sigma_H$
n	Strain hardening coefficient
P	Internal pressure
R	Internal radius of cylinder
r	Vessel radius
t	Plate thickness
v_c	Crack tip displacement
v_c^*	A critical displacement
v_0	Crack center displacement
W	Charpy V-notch energy
β	Coefficient that depends on the material and geometry of the vessel
$\bar{\varepsilon}^*$	True strain at fracture displayed by an unnotched tensile specimen
σ	Nominal stress in a flat plate
$\bar{\sigma}$	Plastic flow stress of a nonstrain hardening material
σ^*	Nominal stress in a flat plate at the onset of crack extension or fracture
σ_H	Hoop stress $\sigma_H = (P \cdot R)/t$
σ_H^*	Critical hoop stress for crack extension
σ_U	Ultimate tensile stress
σ_Y	Yield stress
$\varphi_1, \varphi_2, \varphi_3, \varphi_4, \varphi_5$	Plastic zone correction factors.

Appendix B

Derivation of the plastic zone correction

The major premise of linear elastic-fracture mechanics is that fracture is controlled by a stress or strain (generated within the plastic zone ahead of a crack) which is a function of the single variable K, where $K=\sigma(\pi c)^{\frac{1}{2}}$. The onset of fracture occurs when the stress or strain attains a critical value, which then corresponds to a critical value K:

$$K_c = \sigma^*(\pi c)^{\frac{1}{2}} \tag{B.1}$$

Simple models of a flat plate in simple tension containing a crack with a plastic zone, such as the Dugdale [11] or the Bilby-Swinden model [18], illustrate this property. For example, v_c, the crack-tip displacement, which is closely related to the distortions responsible for ductile fracture [16], [19], can be calculated [19–21]. To simplify matters, a nonstrain hardening material that yields and flows at a stress $\bar{\sigma}$ is treated, and for this material at low stress levels, $\sigma \ll \bar{\sigma}$, the equations reduce to the following expression: [11], [19–22]

$$v_c = B^{-1}K^2\,, \tag{B.2}$$

where $B=2E\bar{\sigma}$. This illustrates that, for a given material, v_c is a function of the single variable K. The critical stress intensity K_c (called the fracture toughness) can then be related to v_c^*, a critical displacement which is independent of nominal stress or crack length*:

$$K_c \equiv (Bv_c^*)^{\frac{1}{2}}\,. \tag{B.3}$$

Both K_c and v_c can be regarded as material properties.

Equation (B.2) is not valid at high nominal stress levels, and must be replaced by the complete solution: [20], [21]

$$v_c = \frac{\sigma^2\pi c}{B}\left(\frac{\pi\sigma}{2\bar{\sigma}}\right)^{-2} \ln\left[\sec\frac{\pi\sigma}{2\bar{\sigma}}\right]^2 \tag{B.4}$$

or

$$v_c = B^{-1}K^2\varphi_3\,, \tag{B.5}$$

where

$$\varphi_3 \equiv \left(\frac{\pi\sigma}{2\bar{\sigma}}\right)^{-2} \ln\left[\sec\frac{\pi\sigma}{2\bar{\sigma}}\right]^2. \tag{B.6}$$

This shows that v_c cannot be expressed only as a function of K at high stresses. This is done by combining (B.3) and (B.4) which gives:

$$K = \sigma(\pi c\varphi_3)^{\frac{1}{2}} \tag{B.7}$$

and

$$K_c = \sigma^*(\pi c\varphi_3)^{\frac{1}{2}}\,. \tag{B.8}$$

In this context, φ_3 can be regarded as a correction factor for large plastic zones. Figure 1 presents φ_3 graphically and illustrates that φ_3 can usually be neglected in the evaluation of K_c when $(\sigma^*/\bar{\sigma}) < 0.6$ (error < 10 percent). Unpublished evidence from this laboratory has shown that φ_3 is a useful plasticity correction for flat plate tests.

An expression for v_0, the crack center displacement—which is where the largest opening is observed—can be derived from the same model [20], [21]:

$$v_0 = \frac{2c\bar{\sigma}}{\pi E}\varphi_5\,, \tag{B.9}$$

where

* A discussion showing the relation between v_c^* and more basic properties of the material is given in [16].

$$\varphi_5 \equiv \ln\left[\frac{1+\sin\dfrac{\pi\sigma}{2\bar{\sigma}}}{1-\sin\dfrac{\pi\sigma}{2\bar{\sigma}}}\right]. \tag{B.10}$$

Combining this with equation (B.2):

$$v_c = v_0\left(\frac{\pi\sigma}{2\bar{\sigma}}\right)^2\frac{\varphi_2}{\varphi_5}. \tag{B.11}$$

This expression can be used to estimate crack-tip displacement values from the crack center displacement measurements.

Appendix C

Summary of flat plate K_c-values for hot-rolled steels

The findings of Nichols *et al.* [4] and Kihara *et al.* [5] are especially useful because their pressure-vessel tests are complimented by flat-plate crack-extension measurements on the same materials. However, these workers did not compute K_c-values. To facilitate comparisons with the K_c-values derived here from their pressure-vessel test, the flat-plate K_c-values have been calculated using φ_3 as the basis for a plasticity correction. The raw data and the results are summarized in Tables C.1 and C.2.

TABLE C.1

Summary of flat-plate crack-extension measurements performed by Nichols et al. [4] *on 1-in.-thick by 84-in.-wide hot-rolled steel plates*

Steel	Test Temp, C	$2c$(in.)	σ^*, psi	$\sigma^*/\bar{\sigma}$	φ_3	K_c, ksi $\sqrt{\text{in.}}$[a]
Ductile crack extension[b]						
A	−30	24	>42,800	0.73	1.36	>305
A	−50	36	>48,000	0.78	1.44	>432
Semibrittle crack extension[b]						
B	16	12	29,100	0.84	1.60	160
B	17	27	18,100	0.52	1.10	124
B	18	24	20,600–23,300	0.64	1.25	141–160
B	47	24	18,100–19,300	0.54	1.15	119–127
C	−19	24	28,000	0.80	1.20	210
C	−20	36	19,900	0.57	1.50	164
C	−25	12	29,800	0.85	1.40	164
C	−46	24	28,900	0.76	1.60	210
Brittle crack extension[b]						
B	−20	24	13,900	0.38	1.0	86
B	−22	12	13,200	0.36	1.0	57

[a] $K_c = \sigma^*(\pi c\varphi_3)^{\frac{1}{2}}$.

[b] Refers to initial model of crack extension.

Steel A: 0.13 C, 1.14 Mn, Al-grain-refined; $\sigma_Y = 40{,}000$ psi, $\sigma_U = 63{,}500$ psi, $\bar{\sigma}$-values based on value derived from pressure-vessel tests at ambient temperatures $\bar{\sigma} = 55{,}000$ psi (see Fig. 5, top), $\bar{\sigma}(-30\text{ C}) \approx 59{,}000$ psi, $\bar{\sigma}(-50\text{ C}) \approx 62{,}000$ psi.

Steel B: 0.36, 0.45 Mn, $\sigma_Y = 34{,}500$ psi, $\sigma_U = 69{,}500$ psi, $\bar{\sigma} = \sigma_Y$ with adjustments made for the temperature dependence of σ_Y.

Steel C: 0.16 C, 1.22 Mn, Si-killed, $\sigma_Y = 31{,}000$ psi, $\sigma_U = 64{,}000$ psi, $\bar{\sigma} = \sigma_Y$ with adjustments made for the temperature dependence of σ_Y.

TABLE C.2

Summay of flat-plate crack-extension measurements performed by Kihara et al. [5] on 19.7-in.-long by 15.7-in.-wide hot-rolled steel plates with 3.14-in.-long edge cracks.

Plate thickness, in.	Test temp, C	σ^*, psi	K_c, ksi $\sqrt{\text{in.}}$[a]
0.25	−118	20,300	73
	−138	18,000	65
	−158	14,500	52
	−170	15,600	56
	−196	8,170	29
0.375	−118	25,200	90
	−138	20,200	73
	−158	15,600	56
	−180	12,400	45
0.500	−118	28,400	100
	−138	23,800	85
	−158	17,000	61
	−180	9,900	36

[a] $K_c = 1.14\,\sigma^*(\pi c)^{\frac{1}{2}}$, no plasticity correction was necessary since $\sigma^*/\sigma_Y < 0.4$ in all cases.

Appendix D

Compilations of pressure-vessel test data

TABLE D 1

Data summary for Anderson and Sullivan [3] for aluminum-alloy vessels

Material properties			Vessel geometry			Test conditions			Calculated values[a]		
Designation	σ_Y, ksi	σ_U, ksi	R, in.	t, in.	R/t	Temp, C	c, in.	σ_B^*, ksi	c^2/Rt	φ_3	$(\sigma_B^{*2}\pi c\varphi_3)^{-1}\times 10^{-10}$ (in.^{3}) (lb.$^{-2}$)
Aluminum 2014-T6	68	79	2.81	0 06	46 8	Room Temp	0.06	64 4	0 02	2.42/1 55	5.29/ 8.26
Ditto	68	79	2.81	0 06	46 8	Ditto	0 25	34 0	0 37	1.2 /1 14	9 17/ 9.66
Ditto	68	79	2.81	0 06	46 8	Ditto	0 50	20 6	1 48	1.13/1 09	13 40/13.76
Ditto	68	79	2.81	0 06	46 8	Ditto	1 00	9.7	5.93	1 08/1.06	31 32/31 91
Ditto	68	79	2.81	0 06	46 8	−196	0 05	71 6	0 014	1 75/1 42	7 09/ 8 74
Ditto	82	93 9	2.81	0 06	46.8	−196	0 07	70 6	0.029	1 74/1.41	5.24/ 6.47
Ditto	82	93 9	2.81	0 06	46 8	−196	0.10	63 7	0.059	1 49/1.31	5.26/ 5.98
Ditto	82	93 9	2.81	0 06	46.8	−196	0 12	58 5	0 085	1 39/1.26	5 57/ 6 15
Ditto	82	93 9	2.81	0 06	46 8	−196	0 15	52.2	0.13	1 29/1 20	6.03/ 6 49
Ditto	82	93 9	2.81	0 06	46 8	−196	0 20	47 4	0.23	1 25/1 17	5 66/ 6 03
Ditto	82	93 9	2.81	0 06	46 8	−196	0 25	40 1	0 37	1 19/1 13	6 65/ 7 00
Ditto	82	93.9	2.81	0 06	46.8	−196	0.37	30.2	0 81	1 14/1.10	8 27/ 8 57
Ditto	82	93 9	2.81	0 06	46 8	−196	0 50	23.1	1 48	1 11/1.08	10 75/11 04
Ditto	82	93.9	2.81	0 06	46 8	−196	0 62	18 6	2.28	1 09/1 07	13 61/13 86
Ditto	82	93 9	2.81	0 06	46.8	−196	0.87	14 4	4 50	1.09/1 07	16 10/16 48
Ditto	82	93.9	2.81	0 06	46.8	−196	1 00	11.3	5 80	1.07/1.05	23.30/23 68
Ditto	90 5	93 9	2.81	0 06	46.8	−253	0.05	82.2	0 014	1 97/1 77	4 78/ 5 32
Ditto	90 5	93 9	2.81	0.06	46.8	−253	0 12	63.4	0 08	1 38/1 34	4 78/ 4 92
Ditto	90 5	93.9	2.81	0 06	46 8	−253	0.25	39.6	0.37	1 16/1 14	6 99/ 7 12
Ditto	90 5	93.9	2.81	0 06	46 8	−253	0 37	32.0	0 81	1 15/1.14	7 30/ 7.37
Ditto	90 5	93 9	2.81	0 06	46 8	−253	0 50	21 0	1.48	1 08/1 08	13.36/13 38
Ditto	90 5	93 9	2.81	0 06	46 8	−253	0 63	19.8	2.35	1 11/1.10	11 60/11 70
Ditto	90 5	93 9	2.81	0 06	46.8	−253	0 87	13.2	4 52	1 08/1.07	19 45/19 63
Ditto	90.5	93 9	2.81	0.06	46.8	−253	1 00	11.9	5 93	1.08/1 08	20 80/20.80

[a] Two values are computed for φ_3 and $\sigma_B^{*2}\pi c\varphi_3$ corresponding to the upper and lower bounds for $\bar{\sigma}$ $\bar{\sigma} = \sigma_Y$, $\bar{\sigma} \simeq \sigma_U$

TABLE D 2

Data summary for Getz, Pierce, and Calvet [9] *for aluminum-alloy vessels*

Material properties			Vessel geometry			Test conditions			Calculated values[a]		
Designation	σ_Y, ksi	σ_U, ksi	R, in.	t, in.	R/t	Temp, C	c, in	σ_H^*, ksi	c^2/Rt	φ_3	$(\sigma_H^{*2}\pi c\varphi_3)^{-1}\times 10^{-10}$ (in.^{3}) (lb^{-2})
Aluminum 2014-T6	90 5	93 9	3 0	0 06	50	−253	0.05	81	0 013	1 86/1 70	5.21/ 5 71
Ditto	90 5	93.9	3.0	0.06	50	−253	0 05	83	0 013	1 97/1 80	4 70/ 5 14
Ditto	9.05	93 9	3 0	0 06	50	−253	0 05	86	0 013	2.54/2.05	3 39/ 4.20
Ditto	9 05	93 9	3.0	0 06	50	−253	0 07	73	0 027	1 53/1 46	5 57/ 5 84
Ditto	90 5	93 9	3.0	0 06	50	−253	0.12	63	0 08	1 36/1 31	4 91/ 5 10
Ditto	90 5	93 9	3 0	0 06	50	−253	0.25	40	0.34	1 14/1 13	6.98/ 7 04
Ditto	90 5	93.9	3 0	0 06	50	−253	0.25	39	0 34	1 13/1 12	7.41/ 7 47
Ditto	90 5	93 9	3 0	0 06	50	−253	0 37	33	0 76	1 12/1 11	7.05/ 7 18
Ditto	90 5	93 9	3 0	0.06	50	−253	0 50	21	1.38	1 06/1 06	13 63/13 63
Ditto	90 5	93 9	3 0	0 06	50	−253	0 61	20	2.06	1 08/1 07	12.08/12.20
Ditto	90 5	93 9	3.0	0 06	50	−253	0 87	14	4.20	1 06/1 06	17 63/17 63
Ditto	90 5	93 9	3 0	0.06	50	−253	1 0	11	5 50	1 05/1 04	25 06/25 18
Ditto	90 5	93 9	3 0	0 06	50	−253	1 0	13	5 50	1 07/1 06	17 63/17 79
Ditto	82.0	93 9	3 0	0 06	50	−196	0 06	70	0 02	1 65/1.40	6 5 / 7 7
Ditto	82.0	93 9	3 0	0 06	50	−196	0 06	72	0 02	1.80/1 45	5 69/ 7.06
Ditto	82.0	93 9	3 0	0 06	50	−196	0 06	75	0 02	2.10/1 50	4 49/ 6.29
Ditto	82.0	93 9	3 0	0 06	50	−196	0 07	72	0.027	1.90/1 45	4 62/ 6 05
Ditto	82.0	93 9	3 0	0.06	50	−196	0 10	65	0 055	1.50/1.35	5 02/ 5 58
Ditto	82.0	93 9	3 0	0.06	50	−196	0.14	60	0 10	1 40/1 30	4.51/ 4 86
Ditto	82.0	93 9	3 0	0.06	50	−196	0 15	54	0 12	1 35/1.20	5 39/ 6.06
Ditto	82.0	93 9	3 0	0 06	50	−196	0.20	45	0.22	1.20/1 15	6 55/ 6.84
Ditto	82.0	93 9	3 0	0 06	50	−196	0 20	50	0.22	1 30/1.20	4 89/ 5 30
Ditto	82.0	93 9	3 0	0 06	50	−196	0 25	39	0 34	1.20/1 10	6 98/ 7 62
Ditto	82.0	93 9	3 0	0 06	50	−196	0.25	41	0 34	1.20/1 10	6.31/ 6 89
Ditto	82.0	93 9	3 0	0 06	50	−196	0 37	30	0.76	1 10/1 10	8 69/ 8.69
Ditto	82.0	93.9	3 0	0 06	50	−196	0 50	23	1 38	1 10/1 07	10 95/11.26
Ditto	82.0	93 9	3 0	0 06	50	−196	1 00	20	5 50	1.05/1 04	30 33/30.60
Ditto	82.0	93 9	3 0	0 06	50	−196	1.00	11	5 50	1 06/1 04	24 89/25 37

[a] Two values are computed for φ_3 and $\sigma_H^{*2}\pi c\varphi_3$ corresponding to the upper and lower bounds for $\bar{\sigma}$ $\bar{\sigma}=\sigma_Y$, $\bar{\sigma}=\sigma_U$

TABLE D 3

Data summary for Duffy et al. [7] *for ductile crack extension in steel pipes*

Material properties			Vessel geometry			Test conditions			Calculated values[a]			
Designation[b]	σ_Y, ksi	σ_U, ksi	R, in.	t, in.	R/t	Temp, C	c, in.	σ_H^*, ksi	c^2/Rt	φ_3	$(\sigma_H^{*2}\pi c\varphi_3)^{-1}\times 10^{-10}$ (in.^{3}) (1b^{-2})	$\sigma^{*-2}\times 10^{-10}$ (in.^{4}) (1b^{-2})
Steel RR, TR, BB	60	80	15	0 375	40	−20–24	0 5	70 6	0.044	∞/2.00	0/0.638	2.00
Ditto	60	80	15	0 375	40	−20–24	0 5	69 8	0 044	∞/2.00	0/0.654	2.05
Ditto	60	80	15	0.375	40	−20–24	1 65	56 2	0 483	∞/1 85	0/0 331	3 16
Ditto	60	80	15	0 375	40	−20–24	1 65	55 8	0 483	∞/1 85	0/0 335	3 20
Ditto	60	80	15	0 375	40	−20–24	2.25	46 8	0 90	∞/1 70	0/0 380	4 50
Ditto	60	80	15	0 375	40	−20–24	2.70	42.6	1.30	∞/1 85	0/0 351	5 50
Ditto	60	80	15	0 375	40	−20–24	3 20	38 8	1 82	∞/2.0	0/0 329	6 64
Ditto	60	80	15	0 375	40	−20–24	4 40	28 2	3.34	∞/1 60	0/0.569	12.50
Ditto	60	80	15	0.375	40	−20–24	4 40	27 8	3.34	∞/1 55	0/0 604	12.90
Ditto	60	80	15	0 375	40	−20–24	4.40	27 6	3 34	∞/1 55	0/0 613	13 10
Ditto	60	80	15	0.375	40	−20–24	4 40	27 6	3 34	∞/1 55	0/0.613	13 10
Steel AF	68	84	15	0 375	40	−16–16	2.65	48.7	1.25	∞/2.20	0/0.230	4 22
Ditto	68	84	15	0 375	40	−16–16	2.65	48 1	1.25	∞/2.10	0/0.247	4 32
Ditto	68	84	15	0 375	40	−16–16	2.65	47 4	1 25	∞/1 90	0/0.281	4 45
Ditto	68	84	15	0.375	40	−16–16	4 40	31 6	3 34	∞/1 75	0/0.414	10 00
Ditto	68	84	15	0 375	40	−16–16	7 50	16 5	10 0	1 9 /1 35	0.82 /1.156	37.20
Ditto	68	84	15	0 375	40	−16–16	10 00	11 4	17 6	1 59/1 25	1 54 /1.96	76 90
Steel AC, AD	53	75	15	0.375	40	2–23	3.5	33.0	2.18	∞/1 65	0/0.506	9 18
Ditto	53	75	15	0 375	40	2–23	3 5	32.8	2.18	∞/1 65	0/0 512	9 30
Ditto	53	75	15	0.375	40	2–23	3 5	32.4	2.18	∞/1 62	0/0 535	9 53
Steel UU	61 7	70	3 06	0 25	12.25	−2–0	2.20	25.3	6 35	∞/∞	0	15 60
Ditto	61 7	70	3 06	0.25	12.25	−2–0	3.55	15 3	16.4	∞/∞	0	42.70
Steel GP	51	73	13	0.281	46.4	17	2.55	37 9	1 78	∞/∞	0	6 90
Steel AH	60	80	18	0.406	45	−8–−4	2.7	43 9	1 0	∞/1.55	0/0 394	5 10
Ditto	60	80	18	0.406	45	−8–−4	2.7	44.7	1.0	∞/1 57	0/0.376	5 00
Ditto	60	80	18	0.406	45	−8–−4	2.7	46 0	1.0	∞/1 65	0/0 337	4 70
Steel YY	62	74	18	0 861	21	62	4 85	33 6	1 50	2.6 /1 5	0.223/0 387	8.80

[a] Two values are computed for φ_3 and $\sigma_H^{*2}\pi c\varphi_3$ corresponding to the upper and lower bounds for $\bar{\sigma}$ $\bar{\sigma}=\sigma_Y$, $\bar{\sigma}=\sigma_U$.
[b] The steels employed in this study are X-50 and X-60 grade line-pipe steels.

TABLE D 4

Data summary for Nichols et al [4] for ductile and semibrittle crack extension in steel, pressure vessels

Material properties			Vessel geometry			Test conditions			Calculated values[a]			
Designation	σ_Y, ksi	σ_U, ksi	R, in.	t, in.	R/t	Temp, C	c, in.	σ_H^*, ksi	c^2/Rt	φ_3	$(\sigma_H^{*2}\pi c\varphi_3)^{-1}\times 10^{-10}$(in.^{3})(lb^{-2})	$\sigma^{*-2}\times 10^{-10}$(in.^{4}(lb.$^{-2}$)
0.36 C Steel[b]	34.5	69 5	30	1.0	30	1–51	3	27.6	0.3	2.3 /1 12	0.6 /1.24	
Ditto	34 5	69 5	30	1 0	30	1–51	3	32.2	0 3	∝/1 16	0/0.88	
Ditto	34.5	69 5	30	1.0	30	1–51	6	18.8	1.2	1.8 /1.09	0 83/1 37	
Ditto	34 5	69 5	30	1 0	30	1–51	6	17.9	1 2	1 62/1 08	1 02/1 53	
Ditto	34.5	69 5	30	1.0	30	1–51	6	21.0	1.2	∝/1.12	0/1 07	
Ditto	34 5	69 5	30	1 0	30	1–51	6	15 9	1 2	1.4 /1 06	1 49/1.98	
Ditto	34.5	69 5	30	1 0	30	1–51	12.37	9 6	5 0	1 5 /1 07	1 86/2.61	
Ditto	34 5	69 5	30	1.0	30	62–88	3	33 0	0.3	—	—	9.8
Ditto	34 5	69.5	30	1 0	30	62–88	6	25.7	1.2	—	—	15.0
Ditto	34 5	69 5	30	1 0	30	62–88	6	27.7	1.2	—	—	13 0
Ditto	34.5	69 5	30	1 0	30	62–88	12	12.7	4.8	—	—	62.0
Ditto	34 5	69.5	30	1 0	30	62–88	12	15.2	4 8	–	—	43.28
Ditto	34.5	69.5	18	1 0	18	10–50	6	13 9	2.0	1.4 /1.06	1 96/2.59	
Ditto	34.5	69 5	18	1 0	18	10–50	6	17 4	2.0	2.15/1 08	0.81/1 62	
Ditto	34 5	69 5	18	1.0	18	79	6	23 4	2.0	—	—	18 2
Ditto	34 5	69 5	57	1.0	57	17	6	22.0	0 63	1.55/1.07	0 7 /1.02	
Ditto	34.5	69.5	57	1 0	57	80	6	27.2	0.63	—	—	13 5
0 13 C Steel[c]	40.0	63 5	30	1 0	30	16–79	6	29.9	1.2	—	—	11.1
Ditto	40.0	63.5	30	1 0	30	16–79	6	31 8	1.2	—	—	9 88
Ditto	40 0	63 5	30	1 0	30	16–79	6	29 4	1.2	—	—	11 56
Ditto	40 0	63 5	30	1.0	30	16–79	6	31.8	1.2	—	—	9.88
Ditto	40 0	63.5	30	1.0	30	16–79	12	19 5	4.8	—	—	26 2
0 16 C Steel[d]	31.0	64.0	30	1 0	30	39	6	28 5	1.2	—	—	13.5

[a] Two values are compured for φ_3 and $\sigma_H^{*2}\pi c\varphi_3$ corresponding to the upper and lower bounds for $\bar{\sigma}\cdot\bar{\sigma}=\sigma_Y, \bar{\sigma}=\sigma_U$.

[b] Plain carbon steel, C 0 36%, Mn · 0 44–0 46%, Si 0 10–0.13% The mode of crack extension in this steel was 100 percent ductile shear above 51 C, semibrittle below 51 C.

[c] Aluminum grain-refined steel, C · 0.13%, Mn · 1.14%, Si 0 12% Crack extension mode was 100 percent ductile shear in all cases.

[d] Silicon-killed steel, C 0.16%, Mn 1 22%, Si. 0.20%. Crack extension mode was 100 percent ductile shear in all cases.

TABLE D 5

Data summary for Kihara, Ikeda, and Iwanga [5] for brittle-steel vessels

Material properties			Vessel geometry			Test conditions			Calculated values		
Designation	σ_Y, ksi	σ_U, ksi	R, in.	t, in.	R/t	Temp, C	c, in.	σ_H^*, ksi	c^2/Rt	φ_3	$(\sigma_H^{*2}\pi c\varphi_3)^{-1}\times 10^{-10}$(in.^{3})(lb^{-2})
Steel[a]	115	125	4.3	0 25	17	−196	2.44	3.98	5 56	1 00	82.64
Ditto	115	125	4.3	0.25	17	−196	1 96	4 95	3 59	1 00	66.22
Ditto	115	125	4 3	0.25	17	−196	1 35	8.25	1 70	1.00	34.6
Ditto	115	125	4.3	0 25	17	−196	0 86	13.2	0 69	1 00	21 17
Ditto	115	125	8 0	0.25	32	−196	3.22	4 95	5 18	1 00	40.48
Ditto	115	125	8.0	0.25	32	−196	2.53	5 60	3 20	1.00	40 16
Ditto	115	125	8 0	0.25	32	−196	1 85	8 52	1 71	1.00	23 69
Ditto	115	125	8 0	0.25	32	−196	1.16	9 60	0.67	1 00	29.76
Ditto	115	125	6 0	0 25	25	−196	1 65	7 56	1 80	1 00	33 78
Ditto	115	125	6 4	0.375	17	−196	2.0	4 40	1 66	1 00	81 96
Ditto	115	125	6 4	0 375	17	−196	2.0	5.70	1.66	1.00	49.01
Ditto	115	125	4.3	0.375	11 4	−196	1 65	7 40	1 68	1 00	35.21
Ditto	115	125	8.0	0.375	21.3	−196	2.24	9 90	1 67	1 00	14 42
Ditto	115	125	4 3	0.50	8.6	−196	2.30	3 42	5 44	1 00	176.0
Ditto	115	125	4 3	0 50	8 6	−196	2.63	3.50	3.20	1 00	99.0
Ditto	115	125	4 3	0.50	8 6	−196	1 94	4.20	1.75	1.00	92.59
Ditto	115	125	4.3	0.50	8 6	−196	1.16	9.20	0.62	1 00	32.46
Ditto	115	125	8 0	0 50	16	−196	3 62	2.40	3.27	1.00	153.8
Ditto	115	125	8 0	0 50	16	−196	2.53	4 80	1 60	1.00	54.64
Ditto	115	125	8.0	0 50	16	−196	1.55	7.20	0 60	1 00	39.68
Ditto	115	125	6.4	0.50	12.8	−196	2.34	4 90	1 71	1 00	56 49

[a] Hot-Rolled Steel, C. 0.25%, Si 0 02%, Mn: 0.85%

TABLE D 6

Data summary for Almond et al. [12] *for ductile-steel vessels*

Material properties			Vessel geometry			Test conditions			Calculated values			
Designation	σ_Y, ksi	σ_U, ksi	R, in.	t, in.	R/t	Temp, C	c, in.	σ_B^*, ksi	c^2/Rt	φ_3	$(\sigma_B^{*2}\pi c\varphi_3)^{-1}\times 10^{-10}$(in.^{3})(lb.$^{-2}$)	$c^{*-2}\times 10^{-10}$(in.^{4})(lb^2)
Steel[a]	45 7	66 0	2.5	0 5	5 0	−25	1.125	32 0	1 01	—	—	9 75
Ditto	45 7	66 0	2.5	0 5	5 0	−25	1 125	35 5	1 01	—	—	7.94
Ditto	45 7	66 0	2.5	0.5	5.0	−25	1 125	36 0	1 01	—	—	7 70
Ditto	47 0	70 6	2.5	0 5	5 0	−5–5	1 125	38 0	1.01	—	—	6.94
Ditto	47 0	70 6	2.5	0 5	5 0	−5–5	1 125	36 5	1 01	—	—	7.50
Ditto	47 0	70 6	2.5	0 5	5 0	−5–5	1 125	35 5	1 01	—	—	7 94
Ditto	49	77	2.5	0 5	5 0	−68	1 125	42 5	1 01	—	—	5 54
Ditto	66	88	2.5	0 5	5.0	−120	1 125	45 7	1 01	—	—	4.80

[a] Hot Rolled Steel, C. 0.14%, Si 0.26%, Mn 0 47%. Crack extension occurred by ductile fibrous mode, at least initially.

TABLE D 7

Data summary for Peters and Kuhn [1] *for aluminum-alloy vessels*

Material properties			Vessel geometry			Test conditions			Calculated values		
Designation	σ_Y, ksi	σ_U, ksi	R, in.	t, in.	R/t	Temp C	c, in.	σ_B^*, ksi	$50(c^2/R^2)\tanh(R/50t)$	φ_3	$(\sigma_B^{*2}\pi c\varphi_3)^{-1}\times 10^{-10}$(in.^{3})(lb^{-2})
Aluminum 2024-T3	36 5	65.0	14 4	0 015	960	Room Temp	0 31	41 3	0 023	∝/1 25	0/ 4 81
Ditto	36 5	65.0	14 4	0.015	960	Ditto	0 64	29 8	0 098	1 74/1 12	3 21/ 4 99
Ditto	36 5	65.0	14 4	0 015	960	Ditto	1 25	20 4	0 37	1 31/1 07	4.67/ 5.71
Ditto	36 5	65 0	14 4	0.015	960	Ditto	2.55	11 3	1 56	1 18/1 04	8.28/ 9 39
Ditto	36 5	65.0	14 4	0 015	960	Ditto	3 85	8 2	3 57	1 18/1 05	10.42/11.71
Ditto	36 5	65 0	3 6	0 025	144	Ditto	0 50	21 9	0 96	2.62/1.15	5.06/11 54
Ditto	36 5	65 0	3 6	0 025	144	Ditto	1 0	10.4	3 84	1 41/1.08	20.85/27 23
Ditto	36 5	65.0	3.6	0 025	144	Ditto	2.81	3 4	29 50	1.25/1 06	78 43/92.48
Ditto	36.5	65.0	3 6	0 015	230	Ditto	0.31	29.3	0 37	∝/1.18	0/10.13
Ditto	36 5	65.0	3 6	0 015	230	Ditto	0 60	17.2	1 38	1 6 /1 11	11.20/16.14
Ditto	36 5	65 0	3 6	0 015	230	Ditto	1 20	8.7	5 50	1.39/1.08	25.24/32.48
Ditto	36 5	65 0	3 6	0 012	300	Ditto	0 49	22.9	0.92	∝/1 16	0/10 68
Ditto	36 5	65 0	3 6	0 012	300	Ditto	1 0	12.8	3 85	2.18/1.14	8.90/17 03
Ditto	36 5	65 0	3 6	0.012	300	Ditto	2.0	5.7	15.40	1.46/1 09	33 57/44 97
Ditto	36.5	65 0	3 6	0.012	300	Ditto	1 90	5 4	13 90	1.32/1.07	43.53/53.7
Ditto	36 5	65 0	3 6	0.012	300	Ditto	0 48	22.8	0 88	2.62/1.15	4.86/11 09
Ditto	36 5	65.0	3 6	0 012	300	Ditto	0.95	10.2	3 48	1 34/1 07	23.99/30 05
Ditto	36 5	65 0	3.6	0.012	300	Ditto	0.28	40.2	0 05	∝/1 24	0/ 5 67
Ditto	36 5	65 0	3 6	0 012	300	Ditto	0.12	41.4	0 05	∝/1 26	0/12.28
Ditto	36 5	65 0	3 6	0 012	300	Ditto	0.25	30 6	0 25	∝/1 16	0/11 72
Ditto	36 5	65 0	3 6	0.012	300	Ditto	0 25	26 4	0 25	1 41/1 11	12.96/16 46
Ditto	36 5	65 0	3 6	0 012	300	Ditto	0 48	20 0	0.80	1 57/1 10	10 56/15 07
Ditto	36.5	65 0	3 6	0 012	300	Ditto	0 93	10 7	3 35	1.37/1 08	21 78/27 63
Ditto	36 5	65 0	3.6	0 012	300	Ditto	1 91	4 9	12.50	1.22/1.66	56 92/65 51
Ditto	36.5	65 0	3.6	0 012	300	Ditto	3 80	2.6	50 0	1 24/1 66	99 56/116 46
Ditto	36 5	65.0	3 6	0 012	300	Ditto	0 48	20 4	0 80	1 62/1 11	9 82/14 34
Ditto	36 5	65 0	3 6	0 012	300	Ditto	0 48	21 0	0 80	1 71/1 12	8 79/13 42
Ditto	36 5	65.0	3.6	0 06	600	Ditto	0.12	44 4	0 05	∝/1 32	0/10 39
Ditto	36 5	65 0	3 6	0 06	600	Ditto	0 23	27 3	0 15	1 56/1.10	11 89/16 86
Ditto	36 5	65 0	3 6	0 06	600	Ditto	0.48	20 7	0.80	1 67/1.11	9.26/13 94
Ditto	36 5	65 0	3 6	0 06	600	Ditto	0 98	10.2	3 50	1 34/1 07	23.32/29 2

TABLE D 8

Data summary for Peters and Kuhn [1] *for aluminum-alloy vessels*

Materials properties			Vessel geometry			Test conditions			Calculated values[a]		
Designation	σ_Y, ksi	σ_U, ksi	R, in.	t, in.	Rt	Temp, C	c, in.	σ_B^*, ksi	$50(c^2/R^2)\tanh(R/50t)$	φ_3	$(\sigma_B^{*2}\pi c\varphi_3)^{-1}\times 10^{-10}$(in^3)(lb^{-2})
Aluminum 7075-T6	65	80	3 6	0 016	225	Room Temp	0 33	19.4	0 40	1.06/1.04	24 68/ 24.65
Ditto	65	80	3 6	0 016	225	Ditto	0 65	11.7	1.60	1 05/1 03	34.08/ 34.74
Ditto	65	80	3 6	0 016	225	Ditto	1 28	5 5	4 50	1.02/1.01	80 60/ 81.43
Ditto	65	80	3 6	0.025	144	Ditto	0 50	16 6	0 50	1 05/1 03	22.01/ 22.44
Ditto	65	80	3 6	0.025	144	Ditto	1.0	8 4	3.90	1 06/1 03	42.57/ 43 81
Ditto	65	80	3 6	0 025	144	Ditto	2.0	3 7	15 50	1 04/1 02	111 84/114 03
Ditto	65	80	14 4	0 016	960	Ditto	0 31	37.2	0.02	2.02/1 39	3 67/ 5 34
Ditto	65	80	14.4	0 016	960	Ditto	0 65	24.9	0 09	1 08/1 05	7 31/ 7 52
Ditto	65	80	14 4	0 017	847	Ditto	1 30	13 6	0 40	1 03/1 02	12.85/ 12.98
Ditto	65	80	14.4	0 017	847	Ditto	2.50	8.5	1 40	1.02/1 01	17.29/ 17 46

[a] Two values are computed for φ_3 and $\sigma_B^{*2}\pi c\varphi_3$ corresponding to the upper and lower bounds for $\bar{\sigma}$: $\bar{\sigma}=\sigma_Y$, $\bar{\sigma}=\sigma_U$.

TABLE D.9

Data summary for Critchlow and Weils [6] for titanium-alloy vessels

Material properties			Vessel geometry[a]			Test conditions			Calculated values[b]		
Designation	σ_Y, ksi	σ_U, ksi	R, in.	t, in.	R/t	Temp, C	c, in.	σ_B^*, ksi	$50(c^2/R^2)\tanh(R/50t)$	φ_3	$(\sigma_B^{*2}\pi c\varphi_3)^{-1}\times 10^{-10}$(in.^{3})(lb^{-2})
Ti-8AC-1Mo-IV	138	149	15	0.05	300	Room Temp	2.25	30 0	1 125	1 06/1.05	1 48/1 49
Ditto	138	149	15	0 05	300	Ditto	3 40	25 0	2.568	1 08/1 06	1.38/1 41
Ditto	138	149	15	0.05	300	Ditto	4.20	19 0	3 920	1 06/1.05	1 98/2.0
Ditto	138	149	15	0 05	300	Ditto	8 0	11 3	14.220	1 07/1 06	2.91/2.94
Ditto	138	149	15	0 05	300	Ditto	9.2	10	18 800	1 07/1 06	3.23/3.26
Ditto	138	149	33.3	0.03	1100	Ditto	2.6	30	0 30	1 02/1 02	1.33/1 33
Ditto	138	149	33 3	0.03	1100	Ditto	5 5	15	1 36	1 02/1 02	2.54/2.54
Ditto	138	149	70	0.03	2325	Ditto	4 25	30	0.18	1.05/1 04	0 79/8 0
Ditto	138	149	70	0 03	2325	Ditto	9.20	15	0 86	1/1	1 53

[a] The $R=15$-in. tests involved cylindrical vessels, the $R=33.3$-in. and 70-in. tests involved curved panels

[b] Two values are computed for φ_3 and $\sigma_B^{*2}\pi c\varphi_3$ corresponding to the upper and lower bounds for $\bar{\sigma}$: $\bar{\sigma}=\sigma_Y$, $\bar{\sigma}=\sigma_U$

TABLE D 10

Data summary for Anderson and Sullivan [3] for titanium-alloy vessels

Material properties			Vessel geometry			Test conditions			Calculated values[a]		
Designation	σ_Y, ksi	σ_U, ksi	R, in.	t, in.	R/t	Temp, C	c, in.	σ_B^*, ksi	$50(c^2/R^2)\tanh(R/50t)$	φ_3	$(\sigma_B^{*2}\pi c\varphi_3)^{-1}$ 10^{-10}(in.^{3})(lb.$^{-2}$)
Ti-5Al-2.5 Sn	193	220	3 0	0 02	150	−196	0 06	190 4	0.02	∝/1 76	0/0 83
Ditto	193	220	3 0	0 02	150	−196	0 12	164.9	0 08	1 90/1 49	0 51/0 65
Ditto	193	220	3 0	0.02	150	−196	0 11	156 6	0 06	1 63/1 38	0 72/0 85
Ditto	193	220	3 0	0 02	150	−196	0.22	115 5	0.26	1 32/1.14	0 82/0 95
Ditto	193	220	3 0	0 02	150	−196	0.23	105 1	0.29	1 26/1 18	0.99/1 06
Ditto	193	220	3 0	0 02	150	−196	0.37	84.9	0.75	1 25/1 18	0.95/1 01
Ditto	193	220	3.0	0 02	150	−196	0 38	74 6	0.80	1 18/1.13	1.27/1 33
Ditto	193	220	3 0	0 02	150	−196	0 47	71 8	1 22	1 24/1 16	1 05/1 13
Ditto	193	220	3.0	0 02	150	−196	0 49	66.2	1 33	1.21/1 14	1.22/1 30
Ditto	193	220	3 0	0 02	150	−196	0 74	44.1	3 00	1.16/1 11	1.90/1 99
Ditto	193	220	3.0	0 02	150	−196	0 73	35.9	2.90	1 09/1 07	3 10/3.16
Ditto	219	240	3.0	0 02	150	−253	0 04	171 5	0 01	1 46/1 34	1 61/1 75
Ditto	219	240	3 0	0.02	150	−253	0 07	160.9	0 03	1 39/1 30	1 14/1.22
Ditto	219	240	3 0	0 02	150	−253	0 09	133 9	0.05	1.23/1.18	1 51/1.58
Ditto	219	240	3 0	0.02	150	−253	0 13	121 4	0 10	1.20/1 16	1.30/1 34
Ditto	219	24	3.0	0 02	150	−253	0.14	114 2	0 10	1 16/1 13	1 50/1 54
Ditto	219	240	3.0	0 02	150	−253	0.26	84 6	0 37	1.11/1.09	1.54/1 56
Ditto	219	240	3.0	0 02	150	−253	0.24	76 0	0 32	1.08/1 06	2.12/2.15
Ditto	219	240	3 0	0 02	150	−253	0.40	63 6	0 88	1 09/1 08	1 79/1 82
Ditto	219	240	3.0	0.02	150	−253	0 47	63.0	1.22	1 13/1 09	1 52/1.55
Ditto	219	240	3 0	0 02	150	−253	0 38	61 5	0.80	1.08/1 07	2.05/2.06
Ditto	219	240	3 0	0.02	150	−253	0 49	51 6	1.33	1 08/1 06	2.25/2.30
Ditto	219	240	3 0	0 02	150	−253	0 80	40.6	3 55	1 11/1.09	2.17/2.21
Ditto	219	240	3 0	0 02	150	−253	0 78	37 7	3.38	1 08/1.07	2.65/2.68

[a] Two values are computed for φ_3 and $\sigma_B^{*2}\pi c\varphi_3$ corresponding to the upper and lower bounds for $\bar{\sigma}$: $\bar{\sigma}=\sigma_Y$, $\bar{\sigma}=\sigma_U$

TABLE D 11

Data summary for Sechler and Williams [10] *for brass vessels*

Material properties			Vessel geometry			Test conditions			Calculated values[a]		
Designation	σ_Y, ksi	σ_U, ksi	R, in.	t, in.	R/t	Temp, C	c, in	σ_R^*, ksi	$50(c^2/R^2)\tanh(R/50t)$	φ_3	$(\sigma_R^{*2}\pi c\varphi_3)^{-1}$ 10^{-10}(in.^{2})(lb.$^{-2}$)
Brass[b]	45	57	1.5	0 001	1500	Room Temp	0 03	50 6	0 02	∞/1 86	0/22.3
Ditto	45	57	1.5	0 001	1500	Ditto	0 04	45 4	0 03	∞/1 52	0/25 4
Ditto	45	57	1 5	0 001	1500	Ditto	0 06	37 1	0 08	1 74/1 71	22.18/29 47
Ditto	45	57	1 5	0 001	1500	Ditto	0 10	30 0	0.22	1'44/1.21	24 53/29 2
Ditto	45	57	1.5	0.001	1500	Ditto	0.10	30 0	0.22	1.44/1.21	24.13/29.2
Ditto	45	57	1 5	0 001	1500	Ditto	0 12	25 5	0 32	1 31/1 16	31 15/35 18
Ditto	45	57	1 5	0.001	1500	Ditto	0.12	25 7	0 32	1 31/1 16	30 65/34.62
Ditto	45	57	1 5	0 001	1500	Ditto	0 13	26.8	0 37	1 39/1 19	24 55/24 68
Ditto	45	57	1.5	0 001	1500	Ditto	0 15	24.0	0 50	1 33/1 17	27.74/31 53
Ditto	45	57	1 5	0 001	1500	Ditto	0 15	21 7	0 50	1 25/1 13	36 03/39 86
Ditto	45	57	1 5	0 001	1500	Ditto	0 17	19.1	0 64	1.20/1 11	42.73/46.2
Ditto	45	57	1.5	0 001	1500	Ditto	0 21	19 1	0 98	1.28/1.15	32.55/36.23
Ditto	45	57	1 5	0 001	1500	Ditto	0 25	14 2	1 38	1 17/1.10	54.09/57.53
Ditto	45	57	1.5	0 001	1500	Ditto	0 30	13 3	2 00	1.21/1 11	49 48/53 94
Ditto	45	57	1.5	0 001	1500	Ditto	0 35	11 0	2.70	1 16/1.09	64 81/68.97
Ditto	40	53.7	2.5	0 001	2500	Ditto	0 032	48 0	0 008	∞/1.86	0/23 17
Ditto	40	53.7	2.5	0 001	2500	Ditto	0 032	46 1	0 008	∞/1 66	0/28 14
Ditto	40	53.7	2.5	0 001	2500	Ditto	0.062	40 0	0.03	∞/1 40	0/22.89
Ditto	40	53.7	2.5	0 001	2500	Ditto	0 094	37.0	0 07	2.6 /1 36	9 52/18.2
Ditto	40	53.7	2.5	0 001	2500	Ditto	0.094	38 7	0 07	∞/1 40	0/16 16
Ditto	40	53 7	2.5	0 001	2500	Ditto	0.10	35.0	0 08	1 98/1.30	13.11/19 98
Ditto	40	53 7	2.5	0 001	2500	Ditto	0 125	32.2	0 12	1 76/1.26	13 96/19 50
Ditto	40	53 7	2.5	0 001	2500	Ditto	0 125	30.2	0 12	1 54/1 21	18 13/23 08
Ditto	40	53 7	2.5	0 001	2500	Ditto	0 15	27 5	0.18	1 44/1 18	19 50/23 80
Ditto	40	53 7	2.5	0 001	2500	Ditto	0.156	26 2	0.20	1 39/1 16	21 41/25 65
Ditto	40	53 7	2.5	0 001	2500	Ditto	0 156	27 0	0.20	1 43/1 18	19 58/23.73
Ditto	52	63 2	2.5	0 003	833	Ditto	0 048	56 4	0 018	∞/1 86	0/11.2
Ditto	52	63 2	2.5	0.003	833	Ditto	0 098	50 0	0.076	∞/1.60	0/ 8.11
Ditto	52	63 2	2.5	0.003	833	Ditto	0 115	48 4	0.10	∞/1 54	0/ 7 67
Ditto	52	63 2	2.5	0.003	833	Ditto	0.125	42.5	0 12	∞/1.54	0/ 9 15
Ditto	52	63 2	2.5	0 003	833	Ditto	0 125	45 0	0 12	2.24/1 44	5 61/ 8.73
Ditto	52	63.2	2.5	0.003	833	Ditto	0 125	43 2	0.12	1.88/1.22	8.25/11 18
Ditto	52	63 2	2.5	0.003	833	Ditto	0 148	41 3	0.17	1 85/1 38	8.10/ 9.13

[a] Two values are computed for φ_3 and $\sigma_R^{*2}\pi c\varphi_3$ corresponding to the upper and lower bounds for $\bar{\sigma}$ $\bar{\sigma} = \sigma_Y$, $\bar{\sigma} = \sigma_U$.
[b] Brass shim stock.

REFERENCES

[1] R. W. Peters, and P. Kuhn, *Bursting Strength of Unstiffened Pressure Cylinders with Slits*, NACA TN 3993, 1957.
[2] E. S. Folias, *Int. J. Fracture Mech.*, 1 (1965) 104.
[3] R. B. Anderson and T. L. Sullivan, *Fracture Mechanics of Through-Cracked Cylindrical Pressure Vessels*, NACA TN D-3252, 1966.
[4] R. W. Nichols, W. H Irvine, A. Quirk and E. Bevitt, *Proc. First Int. Conf. on Fracture*, Sendai, Japan, 1673, 1966.
[5] H. Kihara, K. Ikeda and H. Iwanga, *Brittle Fracture Initiation of Line Pipe*, Document X-371-66, Presented at Int. Inst. Welding, Delft, 1966
[6] W. J. Crichlow and R. H. Wells, *Crack Propagation and Residual Static Strength of Fatigue-Cracked Titanium and Steel Cylinders*, ASTM STP 415, 25, 1967.
[7] A. R. Duffy, *Studies of Hydrostatic Test Levels and Defect Behavior*, Symposium on Line Pipe Research, American Gas Assoc., New York, (1965).
[8] V. Weiss and S. Yukawa, *Critical Appraisal of Fracture Mechanics*, ASTM STP No. 381, 1964.
[9] D. L. Getz, W. S. Pierce and H. Calvert, *Correlation of Uniaxial Notch Tensile Data With Pressure-Vessel Fracture Characteristics*, ASME, 1964.
[10] E. E. Sechler and M. L. Williams, *The Critical Crack Length Pressurized Monocoque Cylinders*, Graduate Aero, Lab. Cal. Inst. Tech. Report, September, 1959. See also M. L Williams in *Proceedings of Crack Propagation Symposium*, Cranfield, (1961) 130.
[11] D. S. Dugdale, *J. Mech. Phys. Solids*, 8 (1960) 100.
[12] E. A. Almond, N. J. Petch A. E. Wraith and E. S. Wright, *The Fracture of Pressurized Laminated Cylinders* (to be published).
[13] J. M. Krafft, *A Rate "Spectrum" of Strain Hardenability and of Fracture Toughness*, Report of NRL Progress, January, 1966. See also G. T. Hahn and A. R. Rosenfield, *ASM Trans.*, 59 (1966) 909
[14] R. G. Forman, *Experimental Program to Determine Effect of Crack Buckling and Specimen Dimensions on Fracture Toughness of Thin Sheet Materials*, AF Flight Dynamics Lab Report AFFDL-TR 65–146, Wright Patterson AFB, Ohio, 1965.

[15] W. G. Degnan, P. D. Dripchak and C. J. Matvsovitch, *Fatigue Crack Propagation in Aircraft Materials*, U.S. Army Aviat. Mat. Lab. Fort Eustis, Va., Technical Report 66–9, March 1966.
[16] G. T. Hahn and A. R. Rosenfield, *Sources of Fracture Toughness. The Relation Between K_{1c} and the Ordinary Tensile Properties of Metals*, ASTM STP 432, 5, 1968.
[17] A. Quirk, *A Maximum Stress Theory for the Failure of Pressure Components Containing Through Thickness Defects*, UKAEA Report AHSB(S) R 134, 1967.
[18] B. A. Bilby and K. H. Swinden, *Proc. Roy. Soc.* A, 285 (1965) 22.
[19] A. A Wells, *Brit. Weld. J.*, 10, 855 (1963).
[20] J. N. Goodier and F. A. Field, *Fracture of Solids* (Edited by Drucker and Gilman), Interscience, New York, 103, 1963.
[21] G. T. Hahn and A. R. Rosenfield, *Acta Met.*, 13 (1965) 293.
[22] A. R. Rosenfield, P. K. Dai and G. T. Hahn, *Proceedings of the First International Conference on Fracture*, T Yokobori, *et al.*, eds., 1 (1966) 223.

RÉSUMÉ

Le mémoire décrit trois critères pour l'extension de fissures axiales traversant de part en part la paroi de récipients sous pression de forme cylindrique. Ces critères sont étroitement liés:

1) Un critère de ténacité à la rupture, applicable surtout aux matériaux à ductilité faible ou moyenne.
2) Un critère basé sur l'écoulement plastique, applicable aux matériaux ductiles.
3) Une adaptation du critère 1 au cas des récipients d'épaisseurs relativement faibles.

L'analyse procède à un couplage entre l'étude théorique par Folias du cas d'une enveloppe cylindrique sous pression, les concepts de résistance à la rupture brutale, et une nouvelle forme de correction plastique. Cette correction, qui est compatible avec des mesures de déplacements à fond de fissure, montre que la contrainte limite d'écoulement plastique gouverne l'extension de fissures de faibles dimensions dans les récipients construits en matériaux ductiles. Par contre, l'extension de fissures plus importantes, ou le cas de matériaux moins ductiles, sont sanctionnés par la ténacité à la rupture brutale. Moyennant une simple adaptation empirique, cette analyse peut être étendue au cas des récipients dont le demi-diamètre est grand vis à vis de l'épaisseur ($R/t > 50$). A cet égard, une estimation des combinaisons critiques entre contrainte de membrane et longueur de fissure peut être déduite de la connaissance du rapport du demi-diamètre à l'épaisseur, et soit de la limite élastique, soit des charges limites d'élasticité et de rupture, soit de K_c. Il n'est pas nécessaire de procéder à un essai préalable en vraie grandeur.

On montre que de telles estimations sont en accord avec les données publiées, qui couvrent des cas de récipients en acier ductile, en acier fragile, en alliages d'aluminium et en alliages de titane.

ZUSAMMENFASSUNG

Diese Abhandlung beschreibt drei nah verwandte Kriterien für die Erweiterung von achsenförmigen Durchrissen in zylindrischen Druckgefäßen.

(1) ein Frakturhärtekriterium besonders für niedrig- und mittelhartes Material,
(2) ein plastisches Zustrom-Spannungskriterium für kurze Risse in harten Materialen, und
(3) eine Modifikation zu (1) für verhältnismäßig dünnwandige Behälter.

Diese Entwicklung verbindet die theoretische Behandlung bei Folias von einer sich unter Druck befindenden Muschel mit der Annäherungsmethode der Frakturstärke und einer neuen Plastizitatsverbesserung. Diese Verbesserung, welche mit den Maßen der Rißspitzenverschiebungen vereinbart ist, zeigt daß die plastische Zustromspannung die Erweiterung von kurzen Rissen in Gefäßen, die aus harten Materialen fabriziert wurden, bestimmt. Dieses steht im Kontrast mit dem Verhalten von längeren Rissen oder spröderen Materialen, welche von der Frakturstärke abhängen. Die Formulierung wurde auf Gefäße mit großem Radius im Verhältnis der Wandstärke, z.B. $R/t > 50$ durch eine einfache, empirische Modifikation, ausgedehnt. Auf diese Art und Weise konnten Schätzungen für Kombinationen der Bandspannungslänge von dem Gefäßradius zum Verhältnis in der Wandstärke und von der gewöhnlichen Gewinnstärke, den Gewinn- und Grundstärken oder K_c ohne frühere, vollständige Testerfahrung erreicht werden. Es wurde gezeigt, daß solche Schätzungen in Übereinstimmung mit der großen Anzahl von veröffentlichten Daten stehen. Eingeschlossen sind biegsame Stahle, spröde Stahle, sowie Aluminium- und Titanlegierungsgefäße.